

ADDIS ABABA UNIVERSITY
SCHOOL OF GRADUATE STUDIES
ENVIRONMENTAL SCIENCE PROGRAMME



**ADSORPTIVE REMOVAL OF FLUORIDE FROM WATER
USING NANO SCALE ALUMINIUM OXIDE HYDROXIDE**

**A Thesis Submitted to the School of Graduate Studies of
Addis Ababa University in Partial Fulfillment of the Requirements for
the Degree of Master of Science in Environmental Science**

By

Fentahun Adeno

March, 2010

ADDIS ABABA UNIVERSITY
SCHOOL OF GRADUATE STUDIES
ENVIRONMENTAL SCIENCE PROGRAM

ADSORPTIVE REMOVAL OF FLUORIDE FROM WATER
USING NANO SCALE ALUMINIUM OXIDE HYDROXIDE

**A Thesis Submitted to the School of Graduate Studies of
Addis Ababa University in Partial Fulfillment of the Requirement for
the Degree of Master of Science in Environmental Science.
Environmental Science Program, Addis Ababa University**

By

Fentahun Adeno Reta

**Advisors: Feleke Zewge (Ph.D)
Yonas Chebude (Ph.D)**

March, 2010

Declaration

I, the undersigned, declare that this thesis is my original work and has not been presented for any degree in any other University and all the resource of material used for the thesis have been duly acknowledged.

Name: Fentahun Adeno Reta

Signature: _____

This Thesis has been submitted for examination with our approval as University advisors.

Name:

Signature

Feleke Zewge (Ph.D)

Yonas Chebude (Ph.D)

Date and place of submission:

Environmental Science Program

Addis Ababa University, March, 2010.

Acknowledgements

During my research work, many people have contributed to my professional as well as personal growth. I wish to take this opportunity to thank all those who assisted me in this research. I am highly indebted to my research advisors, Dr. Feleke Zewge and Dr. Yonas Chebude for their dedicated assistance, consistent guidance, invaluable comments, constant encouragement, indispensable support, constructive criticisms and sharing their rich experience throughout my research work. They should also be acknowledged for providing well established laboratory. I am obliged to them for the confidence they have shown in me and for the patience they have exercised during the research work. Their modern outlook, meticulous supervision as well as cordial cooperation at any moment within the academic routine will always be an example in my life.

I am highly indebted to thank Dr. Yonas Chebude for his cooperation to use a furnace for thermal analysis and Ato H/Gebreal Mengesha for his kind cooperation in using furnace. My thanks also go to Dr. Annette Johnson and Mr. Hermann Moench for characterizing the adsorbent, Swiss Federal Institute for Environmental Science and Technology (Switzerland).

I would like to thank Ato Eyobel Mulugeta for his, thoughtful suggestions, willingness for discussion and sharing his rich experience throughout my research work. I would also like to thank Ato Sahlemicael Deme and Ato Denkew Department of Chemistry, W/t Tigst Mengesha Department of Microbiology, W/t Marta Yishake Environmental Science Program; Addis Ababa University for the technical assistance they gave me during my research work.

Last, but not least, I would like to extend my deepest thanks to my families for their support, encouragement and personal sacrifice showed me for the way of achieving my objective during my research work. Finally, I would like to record deep respect to my friends for their moral support and encouragement

Above all, I wish to thank God for his unlimited blessings.

Table of Contents

Acknowledgements.....	i
List of Figures.....	iv
List of Tables.....	v
Acronyms.....	vi
1. Introduction.....	1
1.1 Backgrounds.....	1
1.2 Environmental Occurrence and Geochemistry of Fluoride.....	2
1.3 Effect of fluoride ingestion in human beings.....	3
1.4 Fluorosis and its Mitigation Options.....	4
1.5 Overview of Defluoridation methods.....	5
1.6 Adsorption Methods.....	6
1.8 Objective.....	11
2. Materials and Methods.....	12
2.1 Defluoridation Material Preparation.....	12
2.2 Characterization of the adsorbents.....	13
2.3 Analytical Methods for the Determination of fluoride ion.....	13
2.3.1 Reagent and Standard Solutions.....	13
2.3.2 Instrumentation.....	14
2.4 Defluoridation Experiment.....	14
2.4.1 Batch Adsorption Studies.....	14
2.4.2 Effect of Dose and Contact Time.....	15
2.4.3 Effect of Thermal Pretreatment.....	16
2.4.4 Effect of Initial fluoride Concentration.....	16
2.4.5 Effect of pH.....	16
2.4.6 Determination of Adsorption Isotherm.....	17
2.4.7 Adsorption Kinetics of Fluoride.....	17
2.4.8 Thermodynamics Study.....	17
3. Results and Discussion.....	18
3.1 Calibration.....	18

3.2 Characterization of the Sorbents	19
3.3 Effect of Adsorbent Dose and Contact Time	22
3.4 Effect of Thermal Treatment	25
3.5 Effect of Initial fluoride Concentration.....	26
3.6 Effect of Water pH.....	27
3.7 Adsorption Isotherm	29
3.8 Adsorption Kinetics of Fluoride.	38
3.9 Intra-particle Diffusion	43
3.10 Mechanism of Adsorption.....	45
3.11 Thermodynamics of Adsorption	46
3.12 Comparison of defluoridation capacities with other adsorbents.....	50
4. Conclusion and Recommendations.....	53
References.....	56

List of Figures

Fig. 1. Calibration curves of five standard solutions.	18
Fig. 2. The X-ray diffraction pattern of nano-AlOOH.....	20
Fig. 3. Residual F ⁻ concentration as a function of time for different dose of nano-AlOOH (C _o = 20 mg/L).	23
Fig. 4. Capacity and efficiency (%) as a function of adsorbent dose (C _o = 20 mg/L, contact time = 60 min, solution).	24
Fig. 5. Effect of thermal treatment on removal efficiency of the adsorbent material (dose = 1.6 g/L, C _o = 20 mg/L, contact time = 60 min).	26
Fig. 6. Effect of initial fluoride concentration on adsorption efficiency as a function of contact time (dose = 1.6 g/L).	27
Fig. 7. Effect of initial solution pH on fluoride removal efficiency of the media (dose = 1.6 g/L, C _o = 20 mg/L, contact time = 60 min).....	28
Fig. 8. Adsorption isotherm of different doses of the adsorbent (dose = 0.4 - 2.0 g/L, C _o = 50 mg/L, contact time = 24 h, pH = 7).	30
Fig. 9. Linearized Freundlich isotherm of the adsorption process (C _o = 50 mg/L, equilibrium contact time = 24 h, pH = 7, temp. = 23 °C).	31
Fig. 10. Linearized Langmuir isotherm of the adsorption process (C _o = 50 mg/L, equilibrium contact time = 24 h, average pH = 7).	33
Fig. 11. Dubinin-Radushkevich equilibrium isotherm model for adsorption of fluoride ion onto nano-AlOOH (C _o = 50 mg/L, pH = 7, temp. = 23 °C).	35
Fig. 12. Temkin equilibrium isotherm model for the adsorption of fluoride ions onto the media, AlOOH (C _o = 50 mg/L, pH = 7.0, temp. = 23 °C).	36
Fig. 13. Adsorption kinetics of fluoride on nano-AlOOH adsorbents at constant surface loading 25 mg/g (average pH = 7).	38
Fig. 14. Pseudo-second-order plot of fluoride adsorption kinetics on adsorbents of different dose each with C _o to adsorbent dose of 40, 20 and 10 mg/L, and 1.6, 0.8 and 0.4 g/L, respectively (with pH of 7.01 - 7.18).....	41
Fig. 15. Average pseudo-second-order plot of fluoride adsorption kinetics on adsorbents each with the same initial load (pH = 7.01-7.18, contact time = 10 h).....	42
Fig. 16. Weber and Morris intra-particle diffusion plot for the removal of fluoride by nano-AlOOH.	44
Fig. 17. Effect of temperature on the removal efficiency of fluoride ion onto nano- AlOOH (Dose = 1.6 g/L, C _o = 20 mg/L, time = 1 h and pH = 7).	48
Fig. 18. Variation of equilibrium constant of fluoride ion sorption with temperature (293 - 313 K) (Dose = 1.6 g/L, C _o = 20 mg/L, contact time = 60 min, pH = 7).	49

List of Tables

Table 1. The trace metal composition of nano-AlOOH which is analyzed by ICP-AES. 21	21
Table 2. Summary of Freundlich, Langmuir, Temkin and D-R isotherm model constants and correlation coefficients for adsorption of fluoride onto nano-AlOOH. 37	37
Table 3. Summary of the Pseudo second-order rate constants, correlation coefficients. . 42	42
Table 4. Change in pH after adsorption process. ($C_0= 20$ mg/L, contact time = 1 h, dose = 1.6 g/L)..... 46	46
Table 5. Thermodynamic parameters for sorption of F^- ion onto AlOOH that are computed from the linearized plot of $\ln K_c$ versus $1/T$ at different temperature. . 50	50
Table 6. Defluoridation capacities and optimum contact time required for the adsorption of fluoride by different sorbents. 51	51

Acronyms

1/bT	Adsorption potential of the adsorbent
AA	Activated alumina
b	Langmuir constant (mg g^{-1})
BC	Bone char
CDTA	Cyclohexyamineldinitrilo tetraacetic acid
C_e	Equilibrium concentration of the adsorbate (mg L^{-1})
C_o	Initial fluoride concentration (mg L^{-1})
CRC	Corporative Research Center
D-R	Dubinin–Radushkevich
E	Mean free energy of sorption per molecule of the sorbate (kJ mol^{-1})
EDTA	Ethylene diamine tetra acetic acid
g	gram
h	hour
ISDWS	Indian Standard Drinking Water-Specifications
ISE	Ion selective electrode
K_a	Adsorption rate constant ($\text{L mg}^{-1} \text{h}^{-1}$)
K_f	Adsorption capacity (mg g^{-1}) based on Freundlich isotherm
kg	kilogram
K_T	Timken isotherm constant (L min mg)
L	liter
m	Mass of adsorbent (g)
mg	milligram
min	minute
mL	milliliter
MoWR	Ministry of Water Resources
n	Freundlich adsorption equilibrium constant (dimensionless)
nm	nanometer
$^{\circ}\text{C}$	Temperature in degree Celsius
ppm	part per million

PXRD	Powder X-ray diffraction
q_e	Amount of solute adsorbed per unit mass of adsorbent (mg g^{-1})
q_m	Langmuir, maximum adsorption capacity (mg g^{-1})
q_s	D-R, maximum adsorption capacity (mg g^{-1})
QSAE	Quality and Standards Authority of Ethiopia
R	Universal gas constant ($\text{kJ mol}^{-1} \text{L}^{-1}$)
sec	Second
T	Absolute temperature (Kelvin)
TISAB	Total ion strength adjustment buffer
USEPA	United State Environmental Protection Agency
WHO	World Health Organization
β	Activity coefficient (mol^2/J^2)
ε	Polanyi potential

Abstract

Fluoride generates effects on skeletal tissues (bones and teeth) and has a narrow range between intakes that cause beneficial and detrimental health effects. Elevated levels of fluoride (>1.5 mg/L) in drinking water supply based on groundwater is a problem in a number of countries and resulting in an increase in the occurrence of dental and skeletal fluorosis in the affected people.

Even though there are numerous effective methods to remove fluoride ion from water most of them are not feasible for developing countries due to their high cost. Adsorption is one of the techniques for the removal of fluoride from water. So far, studies explored the efficiency of various substances such as activated carbon, activated alumina, bone char and clay minerals as adsorbents for the removal of fluoride from water. The most desirable properties of the adsorbent are strong affinity for fluoride and high adsorption capacity.

The present study has concentrated on investigating the fluoride removal potential of nano-scale aluminum oxide hydroxide (nano-AlOOH) produced by controlled precipitation method from aluminum nitrate and ammonium bicarbonate, from aqueous solution. A series of batch adsorption experiments were carried out to assess parameters that influence the adsorption process. The parameters considered were contact time and adsorbent dose, thermal treatment of adsorbent, initial fluoride concentration, pH and water temperature.

Result showed that most of the adsorption took place during the first 30 min; and the adsorption equilibrium reached at one hour contact time with an optimum adsorbent dose of 1.6 g/L for initial fluoride concentration of 20 mg/L. The removal efficiency of fluoride was increased with adsorbent dosage. Fluoride adsorption efficiencies increase with increase in the thermal treatment temperature up to 300 °C, however further increase in temperature resulted in decreased removal efficiency. The fluoride removal efficiency raise as the pH of the solution increase from pH 3 to 8, but further increase in pH the adsorption efficiency decreased; may be due to the hydroxide ion competition

with fluoride ion. Fluoride adsorption capacity increases linearly with increase in fluoride concentration. The adsorption data were well fitted to the Langmuir isotherm model with a maximum capacity of 62.5 mg F⁻/g. The kinetic studies showed that the adsorption reaction of fluoride removal by nano-AlOOH obeys a pseudo-second-order rate equation. Therefore, nano-AlOOH possesses a maximum fluoride adsorption capacity and maximum adsorption occurred at around pH 7 with initial fluoride concentration of 20 mg/L, which makes nano-AlOOH a potential adsorbent for drinking water treatment. The intra-particle diffusion was not a rate-controlling step for the adsorption process. The thermodynamic studies revealed that the adsorption of fluoride by nano-AlOOH was an endothermic and the adsorption process is spontaneous. Thus the adsorbent needs further investigation or characterization in order to initiate projects to conduct pilot study and develop defluoridation unit at different level.

Keywords: *nano-scale AlOOH, Defluoridation, Fluoride removal efficiency, Adsorption capacity, Adsorption kinetics, Adsorption Mechanism.*

1. Introduction

1.1 Backgrounds

Nature gives life to everything by means of water, and is the most precious natural resource that exists on the planet (Ayoob and Gupta, 2006). It is available in abundance in nature covering $\approx 75\%$ of the surface of the earth. The chemical nature of water is one of the most important criterion that determine its usefulness for a particular need, and as such not all the waters are fit for drinking and resulting in shortage of drinking water. Many water sources contain harmful substances that make the water unsafe to drink or unfit for domestic use. As a result, consumption of contaminated water may result in epidemic diseases (Jamode *et al.*, 2004). Water can be contaminated by natural or anthropogenic activities, one such contaminant is fluoride (Pietrelli, 2005).

Ethiopia is one of the countries in the world where the population suffers from the consumption of fluoride rich drinking water (TekleHaimanot Redda *et al.*, 1987; Nemade *et al.*, 2002). According to World Health Organization (WHO) fluoride (F) is a problem for human health if its concentration is above the permissible limit, i.e. 1.5 mg/L (WHO, 1970). However, people residing in the Rift Valley region of Ethiopia are consuming water with fluoride ion concentration much more than the permissible limit. Thus many people are affected by both dental and skeletal fluorosis in the region, where the high fluoride water is the only water source (Reimann *et al.*, 2003).

Most people affected by fluoride contamination in the Ethiopian Rift Valley are poor and rely on underground water as a source of drinking water. Therefore, it is important to

come up with remedial measures, i.e. identify defluoridating methods and adsorbent materials with high rate of fluoride removal.

1.2 Environmental Occurrence and Geochemistry of Fluoride

Fluorine is the 13th most abundant naturally occurring element in the Earth's crust and the lightest member of the halogens. It is a common constituent of most soils and rocks, plants and animals (Tebutt, 1983; WHO, 1999). It has a strong tendency to acquire negative charge, and in solution form found as F⁻ ions, and is found in the earth crust as fluorides (Fawell *et al.*, 2006). Fluoride ions have the same charge and nearly the same ionic radius as hydroxide ions and may replace each other in mineral structures (Feleke Zewge, 2001; Fawell *et al.*, 2006). The average crustal abundance is 0.3 g/kg (Tebutt, 1983), mainly in the form of fluorospar (CaF₂), sellaite (MgF₂), cryolite (Na₃AlF₆), fluorapatite (Ca₁₀(PO₄)₆F₂), and in most soils it is also associated with clay minerals (WHO, 1984; Murray, 1986).

The source of high fluoride concentrations in ground water is primarily associated with: a) addition of fluoride by volcanic activities, b) high water-rock interaction, and c) low calcium concentration. Volcanoes represent the main natural persistent source of fluorine (Symonds *et al.*, 1988). Concentration of fluoride in groundwater depends on many factors, like the geological, chemical and physical characteristics of the aquifer, porosity and acidity of the soil and rocks, temperature, action of other chemical elements, and depth of the wells (Fawell *et al.*, 2006).

From all parts of Ethiopia, the highest levels of fluoride concentrations were found in the Rift Valley region of the country. Fluoride concentrations of the water in the Rift Valley

communities, which are supplied from boreholes, were reported between 1 and 33 ppm (Kloos and Teklehaimanot Redda, 1999) This high fluoride content in the Rift system has been related to volcanoes, high temperature, high subsurface carbon dioxide pressure and low calcium content (Reimann *et al.*, 2003).

1.3 Effect of fluoride ingestion in human beings

Fluoride has a narrow range between intakes that cause beneficial and detrimental health effects (WHO, 2004b). At low concentrations it has beneficial effects on teeth; however excessive exposure to fluoride causes adverse health effects (CRC, 2008). An intake of more than 6 mg fluoride per day will result in fluorosis (Jamode *et al.*, 2004).

Water is the major contributor to the total daily fluoride intake in human body. For that reason, as the concentration of fluoride in drinking water varies, its effect on health also varies accordingly. Thus, fluoride concentration in drinking water, of less than 0.5 mg/L may result in dental caries; in the range of 0.5 - 1.5 mg/L promotes dental health and prevents tooth decay. Further increase in fluoride concentration, (1.5 - 4.0 mg/L) can cause dental fluorosis, in the range of (4 - 10 mg/L) may result in dental as well as skeletal fluorosis and more than 10 mg/L may cause crippling fluorosis (Dissanayake, 1991; WHO, 2004).

The problem of fluorosis has a definite relationship with the following factors: fluoride concentration in drinking water, period of exposure, climatic factors, nutritional status, and exposure from other sources (IPCS, 2002). Drinking water standard for fluoride ion is predetermined by various authorities or/and nations. WHO recommends it in the range of 1.0 - 1.5 ppm (WHO, 2004). The standard of India 1.0 - 1.5 ppm (ISDWS, 1996), U.S

0.5 - 1.5 ppm (US.EPA, 1986) and in Ethiopia 1.5 ppm by Ethiopian Quality and Standard Authority (EQSA, 2001) and 3 ppm by the Ministry of Water Resources (MoWR, 2002). However, people in several region of the Rift Valley of Ethiopia are consuming water with fluoride up to 33 mg/L (Kloos and Teklehaimanot Redda, 1999; Beneberu *et al.*, 2006). Thus the problem of fluorosis is severe and widespread in the region (Reimann *et al.*, 2003), and it is necessary to alleviate the problem by considering different alternatives.

1.4 Fluorosis and its Mitigation Options

Fluorosis is a slow, progressive, crippling problem, and results in health complaints having overlapping manifestations with several other diseases. It is caused by fluoride toxicity (Gopalan *et al.*, 2009). The presence of fluorosis has been known in the Ethiopian Rift valley as early as 1970; however the first literature and sketchy reports came in the mid and late seventies (Olsson, 1979). Consequently, Teklehaimanot Redda *et al.* (1987) studied and reported an extensive epidemiological and clinical survey of endemic dental and skeletal fluorosis including the geochemistry of fluoride. The study shows that the magnitude and seriousness of endemic fluorosis.

The prevention of fluorosis through a range of alternatives is a difficult task, which requires favorable socio-economical conditions of knowledge, motivation, discipline and technique. The possible remedial options to mitigate fluorosis in areas where fluoride concentration is beyond the permissible level may include; 1) provision of alternative source of water, 2) blending high fluoride water with low fluoride containing water, 3) provision of bottled water at least for growing young people, 4) treatment of water supply

(defluoridation) at source and at the point of use, 5) transporting water from a distant source and harvesting rain water etc. Transporting water from distance source needs high initial cost and provision of bottled water, is not economically feasible as in the case most tropical poor developing countries. Therefore, for communities in developing countries like the Rift Valley Regions of Ethiopia where provision of alternative water supply is difficult, treatment is the only option to provide safe drinking water. It is therefore necessary to develop effective defluoridation methods.

1.5 Overview of Defluoridation methods

In drinking water with high concentration of fluoride, defluoridation of water at the point of use or source has to be experienced in order to eliminate any negative effects. Currently wide range of treatment procedures has been reported for the removal of excess fluoride from water. These can be broadly divided into three categories based on mechanism of fluoride removal: precipitation, adsorption and membrane based methods.

Precipitation methods involve the addition of soluble chemicals to the water. Fluoride is removed either by precipitation, co-precipitation, or adsorption onto the formed precipitate. Fluoride removal by chemical precipitation using alum, iron, lime and magnesium compounds, and calcium phosphate was investigated by several researchers (Boruff, 1934; Nawlakhe *et al.*, 1974; He and Cao, 1996; Eva, 2009). Treatment with lime and magnesium makes the water unsuitable for drinking because of the high pH after treatment. The use of alum and lime has been extensively studied for defluoridation of drinking water, and it is popularly known as the *Nalgonda technique* (Nawlakhe *et al.*,

1975). However, it requires much larger dose of alum, low removal efficiency and has problems associated with large sludge disposal (Shrivastava and Vani, 2009).

Defluoridation based on membrane methods is used in developed countries for drinking water treatment. It includes reverse osmosis (Min *et al.*, 1984), nanofiltration (Tahaikt *et al.*, 2007), electrodialysis (Nalan *et al.*, 2008) and electrocoagulation (Sanjeev *et al.*, 2009). It requires more technical support for operation, maintenance and high capital investment cost, high energy consumption and is not selective for fluoride ion removal. Membrane fouling by colloidal material and certain dissolved salts can affect the treatment performance (Feleke Zewge, 2001).

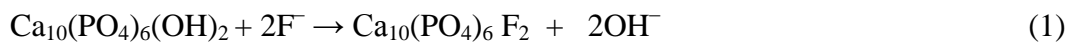
1.6 Adsorption Methods

In adsorption process, the adsorbed solutes are referred to as adsorbate and the adsorbing agent is called adsorbent. Adsorption operations exploit the ability of certain solids preferentially to accumulate specific substances from solution onto their surfaces. A wide range of materials has been tried and studied for fluoride uptake as adsorbent, such as activated alumina, activated carbon, cement paste, aluminum hydroxides, aluminum oxide hydroxide, bone char, various types of clays and red mud etc (Fawell *et al.*, 2006). Some of the most frequently encountered adsorbents used for fluoride up take from water are reviewed below.

Bone Char (BC)

Bone char (BC) is commonly used in developing countries for defluoridation of drinking water. The principal active component of bone char is $\text{Ca}_3(\text{PO}_4)_2$, 57 - 80 %, CaCO_3 6 - 10 % and activated carbon 7 - 10 % (Fawell *et al.*, 2006). Raw BC, prepared from animal

skeletons by calcination at 300 - 600 °C, and the temperature used optimize its properties as a defluoridating agent (He and Cao, 1996). Therefore, BC prepared by heating to 550 °C in low oxygen atmosphere provides good quality adsorbent (Dahi, 2000). The fluoride removal mechanism of BC is believed to be due to its chemical composition, mainly as hydroxyapatite (Fawell *et al.*, 2006; CRC, 2008). The principal reaction is hydroxyl-fluoride exchange of apatite:



The advantage of defluoridation method by BC is; locally available, low cost, Simple and easy to build large scale community plant. However, the drawback of this material is: 1) It may impart unpleasant taste and odor, 2) difficult to predict saturation point and 3) may not acceptable in some countries due to religious cases (Fawell *et al.*, 2006).

Clay

Clay is a sedimentary material composed mainly of fine particles of hydrous aluminum silicates and other minerals and impurities (Fawell *et al.*, 2006). According to different studies on the defluoridation capacity of clay and usability of the method, they reach on different conclusions. However, in general they found that the adsorption capacity of clays was low (CRC, 2008). Thus, Zevenbergen *et al.* (1996) conclude that based on the study the capacity of the ando soil of Kenya was 5.5 mg/g while Girma Moges *et al.* (1996) found that the capacity of ground and fired clay pot of Ethiopia was not more than 0.2 mg/g. Bardsen and Bjorvatn (1997) also studied the sorption capacity of clay calcined at 600 °C and found that, 0.07 mg/g.

Thus the benefits of defluoridation by Clay are: abundant in nature, locally available and relatively low cost. But, the major drawbacks are low capacity and it may also retained toxic heavy metals and wide range of other pollutants in its strata.

Activated Alumina (AA)

Activated alumina is a granular form of aluminum oxide (Al_2O_3). It is prepared by low temperature dehydration ($300\text{ }^\circ\text{C}$ - $600\text{ }^\circ\text{C}$) of aluminum hydroxides (Hao *et al.*, 1986). The crystal structure of alumina contains cation lattice discontinuities giving rise to localized positive charge, and makes alumina to attract various anionic species (Shrivastava and Vani, 2009). Fluoride removal capacities of AA mainly depend on pH. The narrow pH range of 5.5 to 7 is best for efficient removal of fluoride (Pietrelli, 2005). Higher removal at lower pH values due to reduction of negative charges at the surface of AA (Srimurali and Karthukeyan, 2008).

The removal of fluoride from water by adsorption on locally produced hydrated alumina has been also demonstrated by Beneberu Shimelis *et al.* (2005). The result indicated that F^- adsorption is affected by factors such as initial F^- concentration, thermal pretreatment, dose of adsorbent, contact time and the pH of the solution. It was found that the treated adsorbent has a highest fluoride adsorption capacity than the untreated adsorbent, at 1hr contact time and 1.6 g/L dose with minimum removal capacity 23.75 mg/g.

The mechanism of fluoride removal is most probably by ligand exchange reaction at the surface of activated alumina (Hao *et al.*, 1986). Thus fluoride binding to a positively charged or neutral activated alumina can be represented by the following reactions.



Aluminum Oxide Hydroxides

Aluminum oxide hydroxide (AlOOH) exists in many structural forms, boehmite is one of its structural form. It is the major constituent of many bauxite minerals. It can also be synthesized in the laboratory, for instance, by neutralizing inorganic or organic aluminum salts in basic media (Hochepped *et al.*, 2003). It has ion exchange ability, and its hydroxyl group has selective adsorptivity for anions of interest.

The removal of phosphate from water by adsorption onto AlOOH has been investigated by Tanada *et al.* (2003). Rate of adsorption phosphate ion on AlOOH was faster than other adsorbents. The result indicated that the amount of phosphate adsorbed onto AlOOH is influenced by pH, dose of adsorbent, contact time and other competing adsorbate, and conclude that aluminum oxide hydroxide could be used for the removal of phosphate from water. Therefore, a similar pattern of fluoride adsorption onto AlOOH would be expected.

Recently, aluminum oxide hydroxide has shown good adsorption capacity both in batch and packed bed continuous systems on laboratory scale as compared to activated alumina (Beneberu shimelis *et al.*, 2005; Yoseph Abebe, 2007). Conversely, at present nanotechnology has developed quickly in various fields over the past decade and

nanometric material has attracted much attention for its special properties, and has been growing interest in the application of nano particles as sorbents for fluoride.

Thus compared with the traditional micron-sized materials used for separation processes, nano-sized carriers possess a good performance due to the high surface-area to volume ratio and the absence of internal diffusion resistance (Banerjee and Chen, 2007; Wang *et al.*, 2008; Parida *et al.*, 2009). Furthermore, the surface properties, electronic structure, coordination, etc., are modified when the material dimensions reach nano scale. Thus, the nano adsorbents with higher specific surface area have superior adsorption capacity (Wang *et al.*, 2008).

Most atoms on the surface of the nano particles are unsaturated and can easily bind with other atoms. Sundaram *et al.* (2008) studied the defluoridation efficiency of nano-scale hydroxyapatite and showed promising results. Though the removal of fluoride using nano alumina had been reported earlier (Parida *et al.*, 2009) and few reports also describing the potential of nanometer-scale aluminum oxide hydroxide (nano-AlOOH) to remove fluoride from aqueous solutions are available (Wang *et al.*, 2008). Therefore, in this study nano-AlOOH was synthesized in the laboratory scale and used as an adsorbent to remove fluoride from aqueous solutions and investigated the effect of different parameters, such as contact time, dose, initial adsorbate concentration, thermal treatment, pH etc.

1.8 Objective

The general objective of the research was to assess the defluoridation potential of nano size aluminum oxide hydroxide (AlOOH) produced by control precipitation methods.

Specific objectives

The specific objectives of the study were to:

- prepare nano-scale aluminum oxide hydroxide from aluminum nitrate and ammonium bicarbonate;
- determine the crystallinity and size, elemental composition and density of the adsorbent;
- investigate the effect of adsorbent dose, contact time, initial fluoride concentrations and pH of the water on the defluoridating efficiency of the adsorbent;
- investigate the influence of thermal pretreatment on adsorption efficiencies of the adsorbent;
- determine adsorption isotherms of the adsorbent using various models (Freundlich, Langmuir, Dubinin-Radushkevich and Temkin);
- investigate adsorption kinetics of fluoride on the adsorbent;
- examine the mechanism of adsorption;
- study the effect of temperature on sorption character of the adsorbent.

2. Materials and Methods

2.1 Defluoridation Material Preparation

Aluminum nitrate ($\text{Al}(\text{NO}_3)_3 \cdot 9\text{H}_2\text{O}$, 95 %) (Merck), ammonium bicarbonate (NH_4HCO_3 , 98 %) (Merck) and deionized water was used as starting materials. Initially, aluminum nitrate (0.25 M) solution and (0.5 M) solution of NH_4HCO_3 was prepared by dissolving 19.75 g and 46.75 g in 500 ml of deionized water, respectively. Then NH_4HCO_3 and $\text{Al}(\text{NO}_3)_3$ solutions was added (from two separate burettes) to 400 ml deionized water taken in a reaction vessel drop by drop to precipitate Al cations as transparent gel in the form of hydroxides. The mixture was stirred and maintained at 70 °C. Then, pH of the precipitate was maintained in the range of 7.5 to 8.5 using HNO_3 and/or NaOH (Merck, GR). This pH was chosen based on the literature value (Parida *et al.*, 2009). The following chemical reactions occurred during preparation:



The hydrolysis of ammonium bicarbonate in aqueous medium generates OH^- ions by reaction (5). The precipitate obtained by reaction (6) was aged at a temperature of 70 °C for 3 h helped to homogenize the gel due to the slow ripening process. The ageing step is essential to convert $\text{Al}(\text{OH})_3$ to crystalline boehmite by reaction (7). The precipitate were finally filtered, washed thoroughly with deionized water and subsequently with ethanol followed by acetone to avoid contamination of Na ions. The collected precipitate was dried at room temperature and ground to fine powder using mortar.

2.2 Characterization of the Adsorbents.

To identify the phases and crystallinity of the nano-AlOOH, Powder X-ray diffraction (PXRD) pattern of nano-AlOOH were recorded and carried out with PAN analytical X'Pert Pro diffractometer radiation source ($\lambda = 0.1542$ nm). The elemental composition of nano-AlOOH was analyzed using inductive coupled plasma atomic emission spectroscopy (ICP-AES) by digesting in a microwave digester using aqu regia for about 1 h and 20 min. Thus the concentration of the metal element determined from the intensity of light emitted by each metal. The density of nano-AlOOH was also determined by Micro-Meritics AccuPyc 1330, Pycnometer. PXRD, elemental composition and density of nano-AlOOH were determined at Swiss Federal Institute for Environmental Science and Technology, Switzerland through Dr. Feleke Zewge.

2.3 Analytical Methods for the Determination of Fluoride Ion

2.3.1 Reagent and Standard Solutions

A 1000 mg F/L fluoride stock solution was prepared by dissolving 2.21 g of anhydrous sodium fluoride (99.0 % NaF, BDH Chemicals Ltd Poole England) in 1000 ml deionized water in volumetric flask. Standards and samples solutions of fluoride at a required concentration range were prepared by diluting an aliquot of the stock solution, using deionized water. Standard fluoride solutions of 0.5 mg/L, 1.0 mg/L, 5.0 mg/L, 10 mg/L, and 20 mg/L were used for calibrating the instrument.

The total ionic strength adjustment buffer (TISAB) solution was prepared by following a recommended procedure, except that EDTA replaced by CDTA as follows (Bailey, 1980): 57 ml of glacial acetic acid, 58 g of NaCl, 7 g of sodium citrate and 2 g of EDTA

were added to 500 ml deionized water, allowed to dissolve, pH adjusted to 5.3 with 6 M sodium hydroxide, and then made up to 1 L in a volumetric flask with deionized water.

2.3.2 Instrumentation

Fluoride ion was measured by Orion F⁻ ion selective electrode. A pH/ISE meter (Orion Model, EA 940 Expandable Ion Analyzer) equipped with combination fluoride selective electrode (Orion Model 96-09) was employed. The liquid phase fluoride concentration was measured according to the procedure described in the instrument's manual. The method of direct potentiometry was used, where the concentration can be read directly. The fluoride ion selective electrode was calibrated prior to each experiment in order to determine the slope by using fluoride standard solutions. The pH was measured with pH/ion meter (WTW Inolab pH/ION Level 2, Germany) using unfilled pH glass electrode. The meter was calibrated each time measurements were being performed by using pH calibration buffers.

2.4 Defluoridation Experiment

2.4.1 Batch Adsorption Studies

All batch experiments were conducted in 500 ml Erlenmeyer flask containing 500 ml of fluoride spiked deionized water at room temperature (22 ± 2 °C), to evaluate fluoride removal efficiency and capacity of the adsorbent under continuous mixing condition with magnetic stirrer. The effect of dose of the adsorbent, initial fluoride concentration, contact time and raw water pH were investigated by varying any one of the parameters and keeping the other parameters constant. For each trial, a sample was periodically taken out of the flask and filtered through a 0.2 µm filter paper (ADVATEC) for fluoride

analysis. Then, residual F⁻ concentration was measured immediately after equal volume of TISAB was added on 5 ml sample solution. All the experiments were performed in triplicate and the mean values were used.

The adsorption efficiency (%) and the defluoridation capacity (mg F⁻ adsorbed/g of adsorbent) at a given contact time for the selected adsorbents were determined using the following equation (Feleke Zewge, 2001; Beneberu Shimelis *et al.*, 2005).

$$\% \text{ Adsorption} = \frac{(C_o - C_t)}{C_o} \times 100 \quad (8)$$

$$\text{Defluoridation Capacity mg F}^-/\text{g} = \frac{C_o - C_t}{m} \quad (9)$$

Where, C_o and C_t are the F⁻ concentrations initially and at a given time t in mg/L, respectively and m = dose of adsorbent in g/L.

To ensure that F⁻ does not adsorb on the inner walls of the adsorption vessels, blank runs were performed. In this procedure a 20 mg F⁻/L solution was added to a glass vessel and the F⁻ concentration measured after 1 h, 12 h and again after 24 h. Thus no significant reduction in F⁻ concentration was found.

2.4.2 Effect of Dose and Contact Time

To investigate the effect of dose and contact time, experiments were conducted by varying adsorbent dose in the range of 0.4 to 2.0 g/L at constant initial fluoride concentration of 20 mg/L. The dosage range was selected based on Beneberu Shimelis *et*

al., (2005) adsorption test. The residual fluoride concentrations were measured by taking samples at different contact time (5 to 180 min).

2.4.3 Effect of Thermal Pretreatment

To study the effect of thermal treatment on fluoride removal efficiency of the material, each adsorbent heated at different temperatures in a furnace (Calbolite, ELF Model, Waglech International Ltd, UK) for one hour from 50 to 600 °C. At the end of one hour, the thermally treated samples were taken out of the furnace, kept in desiccators and allowed to cool to room temperature. Then, 1.6 g/L of each adsorbent treated at different temperatures were mixed for a contact time of 1 h with 20 mg/L fluoride solution.

2.4.4 Effect of Initial fluoride Concentration

To examine the effect of initial fluoride concentration, experiments were conducted by varying fluoride concentrations ranging from 5 to 30 mg/L at constant adsorbent dose of 1.6 g/L.

2.4.5 Effect of pH

The effect of raw water pH on the adsorption of fluoride onto the media was investigated by varying the initial solution pH range from 2 to 13, were prepared by adjusting the pH to the desired level either with 0.1 M NaOH or 0.1 M HNO₃. Initial fluoride concentrations (20 mg/L), adsorbent dosages (1.6 g/L) and temperature were kept constant during the experiment. The residual F⁻ was determined after 1 h of contact time.

2.4.6 Determination of Adsorption Isotherm

Adsorption Isotherm experiments were conducted to examine the relationship between the solid phase and the solution phase concentration of the adsorbate at an equilibrium condition under constant temperature. Data for plotting isotherm were obtained by mixing a constant F^- concentration of 50 mg/L at pH 7 with adsorbent dose of 0.4, 0.6, 0.8, 1.0, 1.2, 1.4, 1.6, 1.8, and 2.0 g/L. The mixture was agitated for 24 h to ensure equilibrium. A residual fluoride ion was measured and all the values necessary to plot an isotherm were calculated from these determinations.

2.4.7 Adsorption Kinetics of Fluoride

The kinetic analysis of the adsorption data is based on reaction kinetics of pseudo-first-order and pseudo-second-order mechanisms. Adsorption kinetics was determined using constant surface loading of 1.6, 0.8 and 0.4 g/L corresponding to the initial fluoride concentration of 40, 20 and 10 mg/L, respectively. Residual F^- concentrations were measured at different time intervals by taking 5 ml of samples periodically.

2.4.8 Thermodynamics Study

The effect of temperature on the sorption characteristics was investigated by taking 20 mg/L initial fluoride and 1.6 g/L of adsorbent dose of $AlOOH$ at temperatures ranged from 293 up to 313 K.

3. Results and Discussion

3.1 Calibration

The performance of the electrode was checked initially by calibrating using standard solutions of fluoride in the range from 0.5 to 20 mg/L. The electrode potentials of these standard solutions were measured and plotted against the concentration. As can be seen from the Fig. 1 the electrode performance is good, and the slope of the electrode was -58.22 mV, which is almost closer to the theoretical value (-59.2 mV at 25 °C). The standard deviation (SD) was 1.643, which shows good precision.

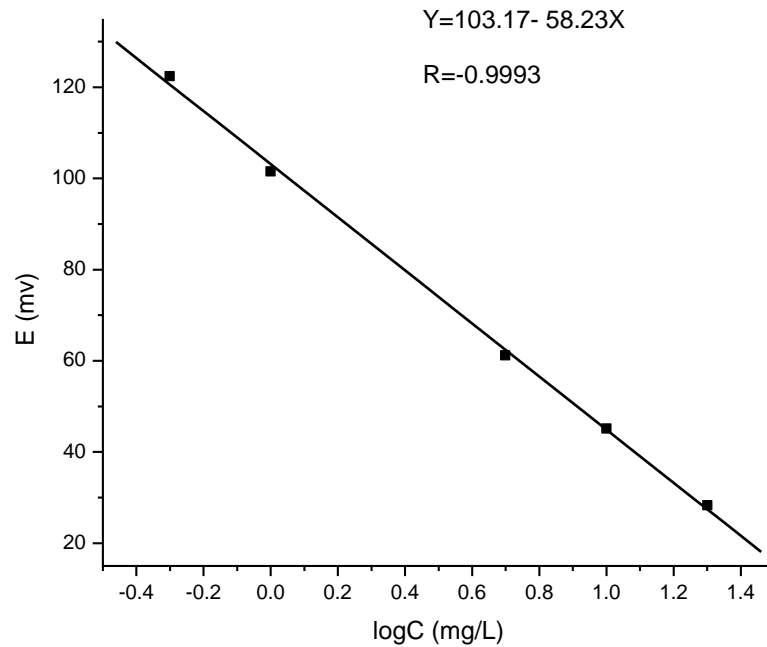


Fig. 1. Calibration curves of five standard solutions.

3.2 Characterization of the Sorbents

Powder X-ray diffraction (PXRD)

The Powder X-ray diffraction (PXRD) pattern of nano-AlOOH were recorded and carried out with PAN analytical X'Pert Pro diffractometer radiation source ($\lambda = 0.1542$ nm). As can be shown in the Fig. 2 different peaks were observed in the XRD powder patterns of the sample for the dried boehmite formed by control precipitation at 70 °C. The result shows a very sharp peaks in the reflection angle range for two theta value (25-30, 35-40, 45-50 and 60-70), which indicates the high crystallinity order of the synthesized compound. This is consistent and matched with PXRD results of nano-AlOOH were done by other researches (Wang *et al.*, 2008; Parida *et al.*, 2009). The boehmite prepared at 70 °C appears to be crystalline in nature, and it seems that control precipitation at 70 °C for 3 h helps to generate crystalline AlOOH due to a slow ripening process. It is very clear that the synthesized AlOOH particles show nano size nature as seen from sharp peak due to the presence of small crystalline sizes. On the other hand the small and broad peak indicating in the range of 10 to 20 angles may suggest the presence of impurities in the synthesized nano-AlOOH sample.

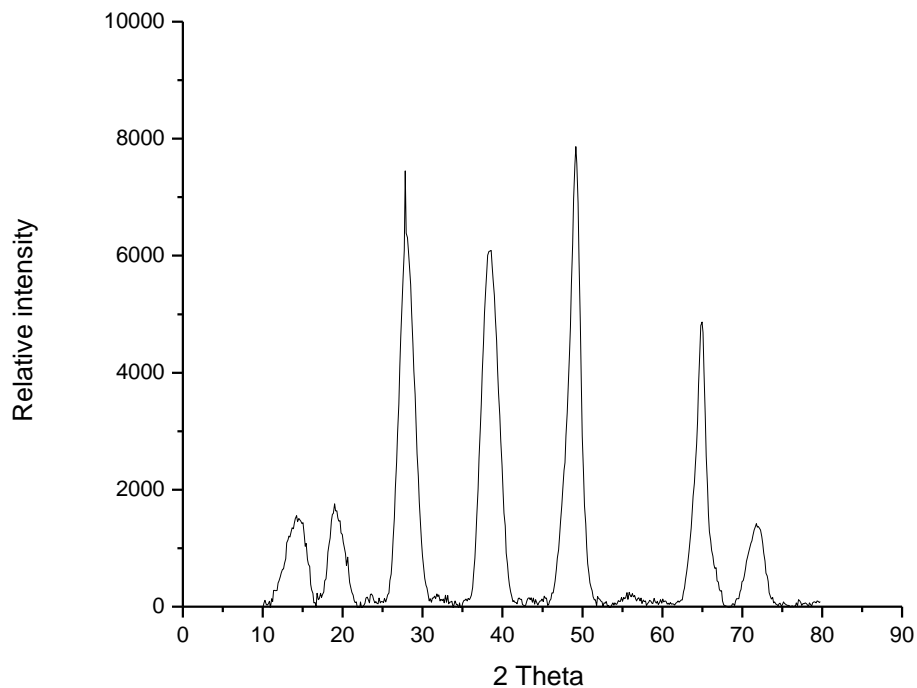


Fig. 2. The X-ray diffraction pattern of nano-AlOOH.

Elemental composition analysis

The elemental composition of the solid phase was determined using inductive couple plasma atomic emission spectroscopy (ICP-AES). ICP-AES, also referred to as inductively coupled plasma optical emission spectrometry (ICP-OES), and is an analytical technique used for the detection of trace metals. It is a type of emission spectroscopy that uses the inductively coupled plasma to produce excited atoms and ions that emit electromagnetic radiation at wavelengths characteristic of a particular metal element (Stefansson *et al.*, 2007). The intensity of this emission is an indicative of the concentration of the metal element within the sample and can be converted to an elemental concentration by comparison with calibration standards. Thus the elemental composition determined by ICP shows that the major component of the solid phase of the

sample was aluminum and accounts 356.33 mg/g. The elemental composition analysis also provides other trace elemental components of the sample, such as Ca, Pb, Na, Si, Al, K, Fe, Se, Sr, Cu, Cd, Zn, Ni, Co, Cr, Mn, Mo, As and Mg as shown in Table.1. Generally, from all metal analyzed next to aluminum Calcium, sodium and potassium were found in large amounts as compared to other elements. The presence of high amount of sodium metal possibly from the NaOH solution used to adjust the pH during synthesis of nano-AlOOH. However, the presence of large amount of calcium possibly from the raw material used to prepare the sample or due to contamination of the sample. Even though calcium helps for reduction of fluoride ion in water through precipitation, to keep the quality of the adsorbent media further chemical characterization of the adsorbent as well as the raw materials is required. The rest of the metal elemental analyzed was found with trace levels averagely below 0.5 mg/g. On the other hand Si, Sr, Cd, Ni, Mn and Mg are found below the detection limit (DL) of the instrument.

Table 1. The trace metal composition of nano-AlOOH which is analyzed by ICP-AES.

N_o	Metals	Concentration (mg/g)	N_o	Metals	Concentration (mg/g)
1	Na	7.46	10	Cu	0.25
2	Ca	8.80	11	Cd	< DL
3	Pb	0.20	12	Zn	0.19
4	Si	< DL	13	Ni	< DL
5	Al	356.33	14	Co	0.10
6	K	2.51	15	Cr	0.06
7	Fe	0.56	16	Mn	< DL
8	Se	1.27	17	Mg	< DL
9	Sr	< DL			

Density determination

The density of nano-AlOOH was determined by Micro Meritics AccuPyc, 1330, Pycnometer. The sample was first kept in a furnace at 110 °C for overnight to remove the

moisture absorbed in it. Then, the Pycnometer provides the density of nano-AlOOH by measuring the sample volume from the amount of displaced gas (helium) and by incorporating the sample mass, from an external measurement. Thus the density of nano-AlOOH was obtained 2.18 g/cm^3 , and is smaller than the density of boehmite, 3.01 g/cm^3 (Wefers and Misra, 1987). Based on the result it can be concluded that the lower density of nano-AlOOH indicates the materials might have more pore spaces, and this poses nano-AlOOH makes nano-AlOOH an effective defluoridating agent.

3.3 Effect of Adsorbent Dose and Contact Time

The effect of adsorbent dose and contact time on the fluoride removal efficiency of AlOOH was studied by varying mass of adsorbents ranging from 0.2, 0.4, 0.6, 0.8 and 1.0 g at constant initial fluoride concentration of 20 mg/L. The results are shown in Fig. 3. The result shows that the reaction was very fast during the initial 30 min, and a contact time of about 60 min is enough to remove more than 95 % of the fluoride in solution with an adsorbent dose greater than or equal to 1.6 g/L. This indicates that longer contact time has no effect under the condition specified above.

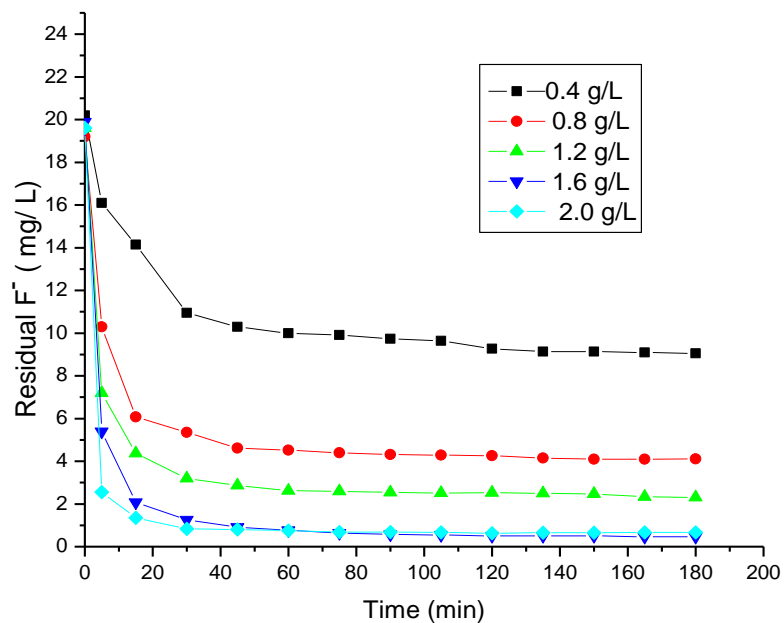


Fig. 3. Residual F⁻ concentration as a function of time for different dose of nano-AlOOH (C₀ = 20 mg/L).

The defluoridation efficiency (%) was significantly increased with dose as reflected by the measured residual fluoride concentration (Fig. 3). The percent removal of fluoride increase significantly up to adsorbent dose of 1.6 g/L, however no significant change was observed beyond this dose under the experimental condition used. Therefore, further increase in the dose result in too much production of sludge and wastage of material. The increase in fluoride adsorption efficiency was due to the large number of available F⁻ binding sites resulting from the increased in adsorbent dosage. Thus, 1.6 g/L of adsorbent dose and 60 min was taken as an optimum dose and contact time for further experiments.

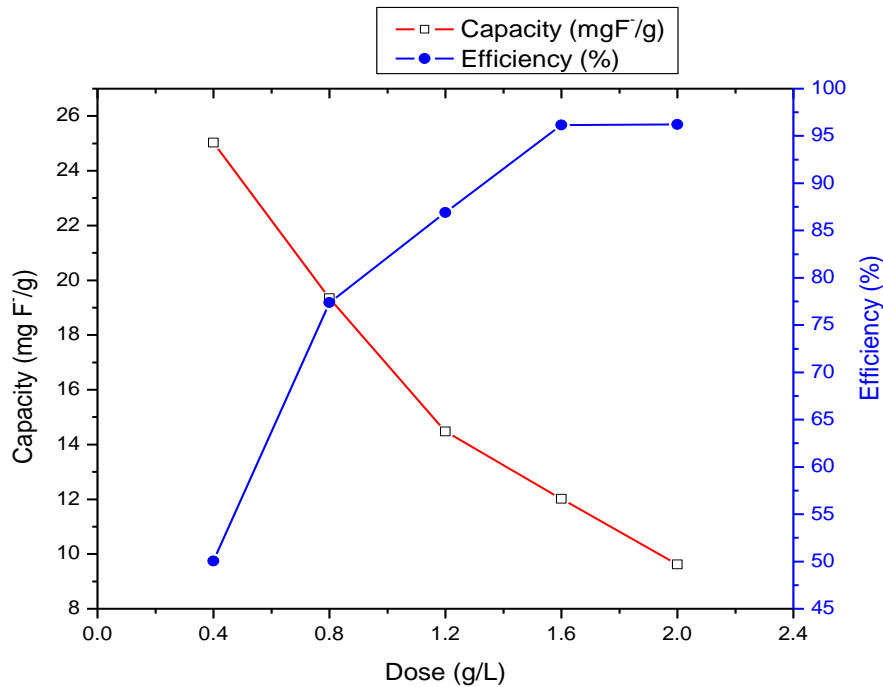


Fig. 4. Capacity and efficiency (%) as a function of adsorbent dose ($C_o = 20$ mg/L, contact time = 60 min, solution).

Conversely, the adsorption capacity decreases with increasing dose (Fig. 4). To maintain maximum capacity and high removal efficiency, the surface loading (i.e., the mass ratio of fluoride to adsorbent dose) should be lower than the optimum value (i.e., the surface loading for optimum fluoride removal, about 90 %, obtained from Fig. 4 is 13.25 mg/g or less). A dose of 1.6 g/L corresponding to the capacity of about 11.88 mg F⁻/g of adsorbent was considered for further adsorption experiments, which is greater than the reported surface loading of micronized AlOOH (11.25 mg F⁻/g of adsorbent) for the corresponding dose of 1.6 g/L (Beneberu Shimelis *et al.*, 2005).

3.4 Effect of Thermal Treatment

Figure. 5 shows, change in the fluoride removal efficiency as a function of adsorbent thermal treatment temperature. The fluoride adsorption efficiencies of the media do not show a significant change when the material is heated to a temperature of 300 °C. The relative increasing F⁻ removal efficiency up to 300 °C may be due to the removal of physically adsorbed water molecule. However, further increase in temperature resulted in decreased removal efficiency. The decrease in fluoride removal efficiency may caused by surface modification and/or change in the composition of the adsorbent, but it requires further study on characterization of the materials. Moreover, heat treatment may remove hydroxyl groups from the surface, and may decrease the number of reactive sites (worku Negussie *et al.*, 2007). The fluoride removal efficiency was high relatively for the adsorbent treated at 200 °C and 300 °C. Therefore, the adsorbent treated at 200 °C and 300 °C have almost closer and significant removal efficiency (about > 94 %). From the removal efficiency, energy expenditure and cost effectiveness the adsorbent treated at 200 °C was selected for further study.

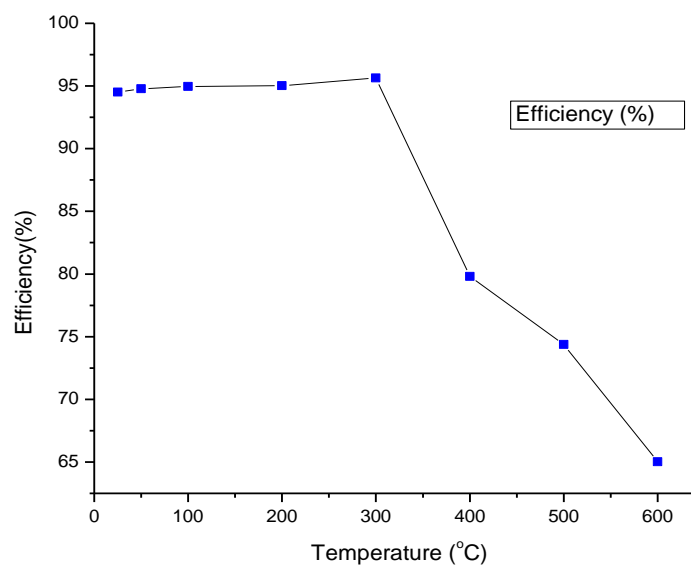


Fig. 5. Effect of thermal treatment on removal efficiency of the adsorbent material (dose = 1.6 g/L, $C_o = 20$ mg/L, contact time = 60 min).

3.5 Effect of Initial fluoride Concentration

The effect of initial fluoride concentrations on the adsorption of fluoride were studied by varying the initial fluoride concentrations at constant contact time and adsorbent dose. As clearly shown in Fig. 6, the efficiency increases with decreasing initial fluoride concentration at the initial stage of adsorption. It can be observed that the adsorption of fluoride from water is relatively more rapid at lower initial concentrations. This is due to the utilization of more accessible energetically active site on the adsorbent surface. Thus the initial fluoride concentration had an influence on the equilibrium sorption time, and significant fluoride removal efficiency (>90 %) was observed when the initial fluoride was less than or equal to 20 mg/L for a contact time of 60 min. For a lower initial fluoride concentration (e.g. 5 mg/L) significant amount of fluoride was removed within 5 min.

Since, the adsorption of more concentrated initial solution approached equilibrium slowly. This indicates that at a given contact times and adsorbent dose initial adsorbate concentration also has much significance effect on fluoride adsorption efficiency.

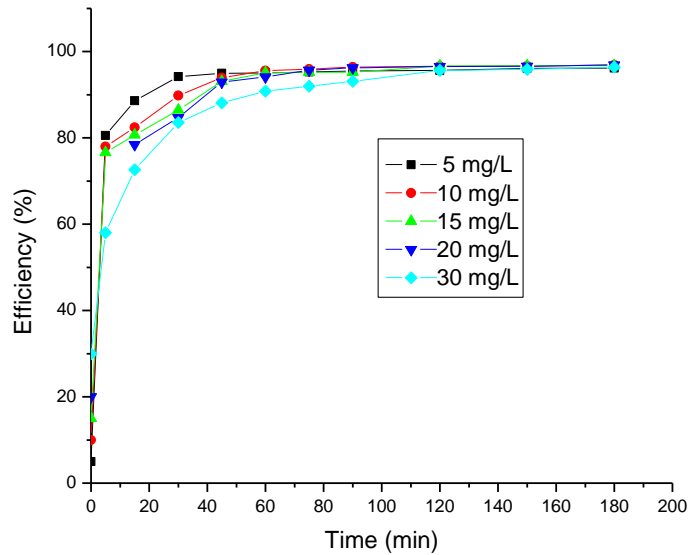


Fig. 6. Effect of initial fluoride concentration on adsorption efficiency as a function of contact time (dose = 1.6 g/L).

3.6 Effect of Water pH

Fig. 7 shows the influence of initial solution (raw water) pH on the fluoride removal efficiency of the adsorbent. As literature reveals that pH of the solution significantly affect fluoride uptake capacity (Venkobachar *et al.*, 1997; Beneberu *et al.*, 2005). It is evident that percentage of fluoride removal increase as the pH of the solution increase with in pH range of 2 to 8 and reach in maximum at pH = 7. Further increase the solution pH from 8 to 13 decreases the removal efficiency and it becomes significant after pH of 9. This is consistent with the work of Wang *et al.* (2008) and Parida *et al.* (2009). The

experimental results showed that the fluoride uptake capacity of this media is more favored with in pH range of 6 to 8, possibly due to the development of positive sites at the surface of the adsorbent. The decrease in the fluoride removal below pH 5 is possibly due to the protonation of the fluoride ion. On the other hand, at a pH above 8, fluoride removal efficiency decreases possibly due to the development of negative charge on the adsorbent surface and/or stronger competition from hydroxide ions. Since both OH^- and F^- have the same charge and ionic radii (Beneberu *et al.*, 2005; Fawell *et al.*, 2006). This is consistent with the study of Wang *et al.* (2008); Nano- AlOOH has a pH_{pzc} of 7.8, which means that the surface of the adsorbent presents a net positive charge when $\text{pH} \leq 7.8$. Therefore, the high efficiency in pH less than 8 can be attributed to the gradual increase in attractive forces, and low efficiency in alkaline medium can be explained by the repulsion between the negatively charged surface and fluoride. Therefore, the extent of adsorption of fluoride ion on nano- AlOOH is governed by the pH of the solution.

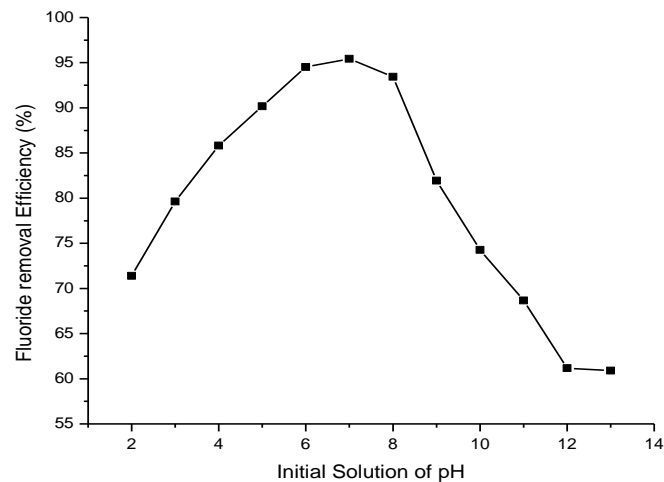


Fig. 7. Effect of initial solution pH on fluoride removal efficiency of the media (dose = 1.6 g/L, $C_o = 20$ mg/L, contact time = 60 min).

3.7 Adsorption Isotherm

An adsorption isotherm is a graphical representation expressing the relation between the mass of fluoride ion adsorbed at constant temperature per unit mass of adsorbent and liquid phase fluoride ion concentration at equilibrium. Adsorption isotherms have many important practical implications; such as they provide information on how adsorption system proceeds, and indicate how efficiently a given adsorbent interacts with adsorbate.

The isotherm experiments were carried out at 9 different dosages of the adsorbents in a range from 0.4 to 2.0 g/L. Fig. 8 shows an adsorption isotherm, which indicates the relationship between the bulk aqueous phase concentration of adsorbate and the solid phase concentration (i.e. the amount of adsorbate adsorbed per unit mass of adsorbent) at an equilibrium condition under constant temperature (22 ± 2 °C). As can be seen from Fig. 8 the adsorption capacity increases with decrease in adsorbent dose and increase in bulk phase concentration at equilibrium. This can be attributed to the utilization of less accessible or energetically less active sites because of increase in diffusivity and activity of fluoride with increase in fluoride concentration (Worku Negussie *et al.*, 2007). Thus the resistance force to the pore diffusion is overcome and the adsorption sites present on the interior surface of a pore might be easily accessible thereby increasing the adsorption capacity. Since the adsorption site become less difficult to the adsorbate upon increasing concentration.

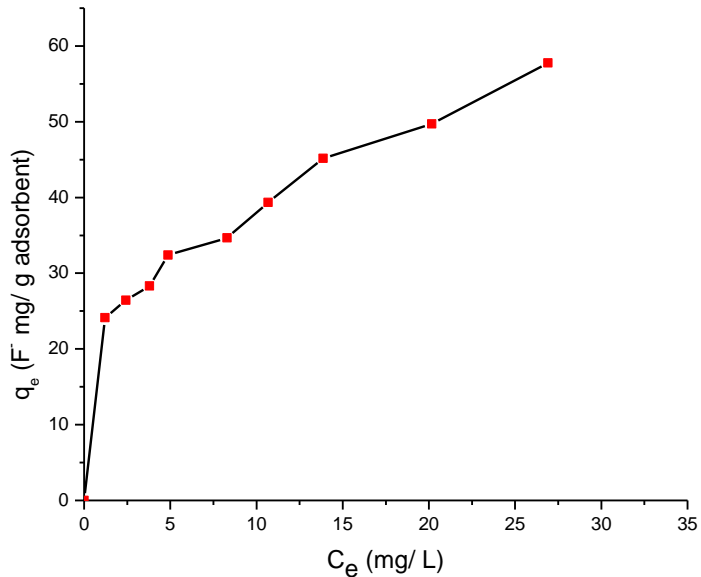


Fig. 8. Adsorption isotherm of different doses of the adsorbent (dose = 0.4 - 2.0 g/L, $C_o = 50$ mg/L, contact time = 24 h, pH = 7).

In order to get additional information about the fluoride adsorption characteristics, the experimental data of equilibrium isotherm for F^- ions adsorption by the adsorbent were modeled using the most frequently used isotherms, such as Freundlich, Langmuir, Dubinin–Radushkevich (D - R) and Temkin isotherm.

Freundlich isotherm

Freundlich isotherm assumes unlimited sorption sites which correlated better with heterogeneous surface of the adsorbent media (Bailey, 1980). The Freundlich equation represented as follows in both general and linearized form, respectively.

$$q_e = K_f C_e^{1/n} \quad (10)$$

$$\log q_e = \log K_f + \frac{1}{n} \log C_e \quad (11)$$

Where, q_e is the adsorbed fluoride at equilibrium per unit mass of adsorbents (mg/g), K_f is the minimum sorption capacity (mg/g) and $1/n$ is the adsorption intensity. C_e is the equilibrium concentration of fluoride (mg/L).

From the experimental data the Freundlich parameters along with correlation coefficients were obtained by plotting $\log(q_e)$ vs. $\log(C_e)$ Fig. 9. The Freundlich constants K_f and $1/n$ of the adsorption isotherm was 20.75 and 0.286 respectively, and it is found that the related correlation coefficient R^2 value for the Freundlich model is (0.9778). The low value of $1/n$ (less than 1) indicates the favorable condition of the adsorptions. Hence, Freundlich isotherm is a good model for defluoridation using the media (nano- AlOOH).

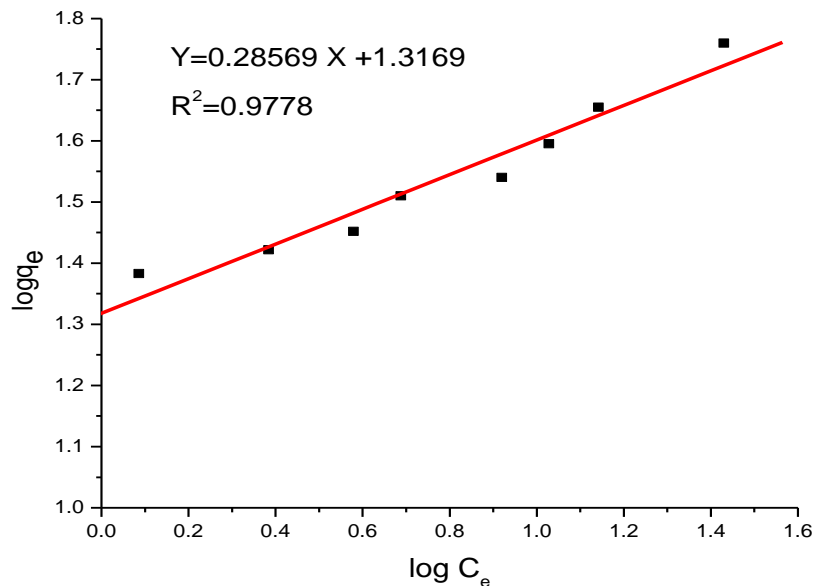


Fig. 9. Linearized Freundlich isotherm of the adsorption process ($C_o = 50$ mg/L, equilibrium contact time = 24 h, pH = 7, temp. = 23 °C).

Langmuir isotherm

Monolayer adsorption can be described by Langmuir equation. The model assumes a monolayer adsorption onto a surface containing a finite number of adsorption sites with uniform energy of adsorption and a single layer of adsorbed solute at a constant temperature (Weber and Chakkravorti, 1974). The Langmuir equation presented below in general and linearized form, respectively:

$$q_e = \frac{q_m b C_e}{1 + b C_e} \quad (12)$$

$$\frac{C_e}{q_e} = \frac{1}{q_m b} + \frac{C_e}{q_m} \quad (13)$$

Where, C_e is the equilibrium concentration of the adsorbate (mg/L), q_e is the adsorbed adsorbate at equilibrium per unit mass of adsorbents (mg/g), q_m and b are Langmuir constants related to adsorption capacity and energy of adsorption process, respectively.

Langmuir isotherm is useful for the estimation of maximum adsorption capacity corresponding to complete monolayer coverage. The plot of specific sorption (C_e/q_e) against the equilibrium concentration (C_e) for F^- ions is shown in Fig. 10. The sorption capacity, q_m , which is a measure of the maximum adsorption capacity corresponding to complete monolayer coverage, is 62.50 mg/g. The adsorption coefficient, b that is related to the apparent energy of sorption for F^- onto AlOOH is $2.25 \times 10^{-1} \text{ L mg}^{-1}$, and finally it was found that the related correlation coefficient R^2 value is near to unity (0.9822). This indicated that the Langmuir model give a good fit to the sorption process.

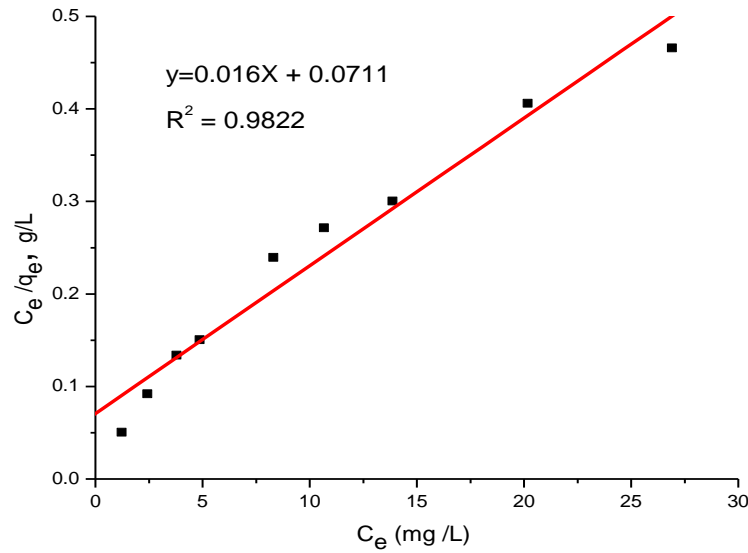


Fig. 10. Linearized Langmuir isotherm of the adsorption process ($C_o = 50$ mg/L, equilibrium contact time = 24 h, average pH = 7).

Dubinin–Radushkevich (D-R) isotherm

Even if the Freundlich and Langmuir isotherm models are widely used, they do not provide any idea about the adsorption mechanism. Thus, to describe the mechanism of adsorption process, the equilibrium data was tested with D-R isotherm model. The D-R model is used to estimate both of the maximum adsorption capacity and the apparent energy of adsorption to distinguish between chemical and physical types of adsorptions. The D-R isotherm assumes a fixed sorption space close to the sorbent surface where sorption takes place. It describes heterogeneity of sorption energies within this space, independent of temperature. The model represented by the equation below:

$$\ln q_e = \ln q_s - \beta \varepsilon^2 \quad (14)$$

Where, q_e and q_s are sorbed concentration and maximum sorption capacity (theoretical saturation) respectively at the sorbent surface, expressed in units of mg/g and, β is a

constant related to mean free energy of the adsorption, in units of $(\text{mol}^2/\text{J}^2)$ and ϵ is Polanyi potential, is the work required to remove a molecule or ion away from its location in the sorption space. It is calculated as:

$$\mathcal{E} = RT \ln\left(1 + \frac{1}{C_e}\right) \quad (15)$$

Where, R is the universal gas constant ($R=8.314 \text{ J/K.mol}$), T is the temperature in Kelvin and C_e is the equilibrium concentration of sorbate in solution.

When $\ln q_e$ is plotted against ϵ^2 , a straight line may be obtained if the sorption data follow the D-R isotherm. The mean free energy of adsorption per molecule of the sorbate E , is the energy required when the adsorbate migrates to the surface of the adsorbent from infinite distance in the solution to the sorbent surface. Thus it can be correlated and calculated from the β value by using the relation (Hobson, 1969):

$$E = \left(\frac{1}{\sqrt{2\beta}}\right) \quad (16)$$

Fig. 11 shows a plot of $\ln q_e$ vs. ϵ^2 , provided straight line plot for the adsorption of fluoride onto the adsorbent. Examination of the experimental data indicates that the D-R isotherm also provides a good fit and description of the data for the fluoride ions adsorption over the concentration range studied. The adsorption processes have adsorption energy values of $13.15 \text{ kJ mol}^{-1}$ for F^- ions onto nano- AlOOH . If the magnitude of free energy of adsorption is between 8 and 16 kJ/mol, the adsorption process corresponds to chemical ion-exchange type, and the value of $E < 8 \text{ kJ/mol}$ represents a physical adsorption (Rieman *et al.*, 1970; Kiran *et al.*, 2006). The energy value for fluoride ions sorption onto nano- AlOOH indicates that the sorption process is predominantly chemical ion-exchange in nature.

The sorption capacity, q_s in the D-R equation was found to be 112.80 mg/g for F^- sorption on AlOOH. The related correlation coefficient R^2 also found 0.9754, and this indicated that a good fit of the isotherm to the experimental data.

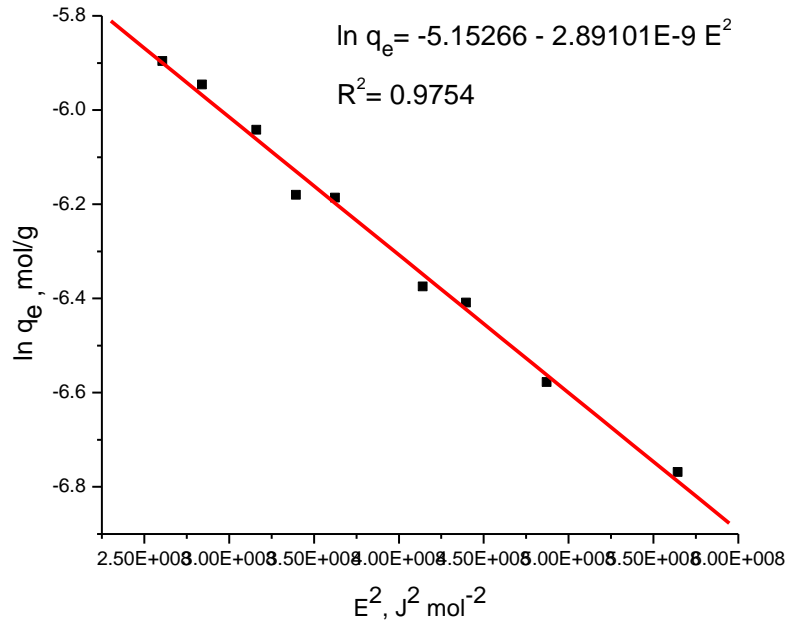


Fig. 11. Dubinin-Radushkevich equilibrium isotherm model for adsorption of fluoride ion onto nano-AlOOH ($C_o = 50$ mg/L, pH = 7, temp. = 23 °C).

Temkin isotherm

Temkin adsorption isotherm model was chosen to evaluate the adsorption potentials of the adsorbent for adsorbates. The model considers the effects of indirect adsorbate/adsorbent interactions on adsorption isotherms. The heat of adsorption of all the molecules in the layer would decrease linearly with coverage due to adsorbate/adsorbent interactions. The Temkin isotherm equation presented as follows in general and linearized form respectively:

$$q_e = \frac{RT}{b_T} \ln K_T C_e \quad (17)$$

$$q_e = \frac{RT}{b_T} \ln KT + \frac{RT}{b_T} \ln C_e \quad (18)$$

Where $1/b_T$ is the adsorption potential of the adsorbent; and K_T is the Temkin isotherm constant.

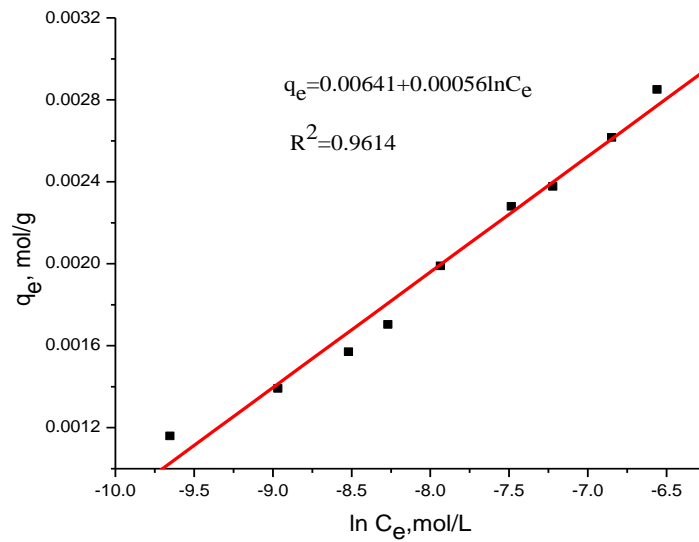


Fig. 12. Temkin equilibrium isotherm model for the adsorption of fluoride ions onto the media, AlOOH ($C_o = 50$ mg/L, pH = 7.0, temp. = 23 °C).

Fig. 12 shows the Temkin isotherm plot for the adsorption of fluoride ions onto nano-AlOOH. The Temkin constant, K_T , of the media (AlOOH) for F^- are 92.75 L/ mg. The Temkin adsorption potential, $1/b_T$, related to heat of sorption for the fluoride ions onto the adsorbent expressed as RT/b_T was 0.00056 for nano-AlOOH.

The Temkin isotherm described the experimental data successfully with R^2 values 0.9614. Though, the plots $\ln C_e$ vs. q_e remains most frequently curvilinear (yoseph Abebe, 2007). In this study, the plots were also found to be near curvilinear. Even though non-linearity of plots for fluoride adsorption experiments, the model considered to be convenient because the curves come close to linearly over a wide range of concentration (Bache and Williams, 1971).

Table 2. Summary of Freundlich, Langmuir, Temkin and D-R isotherm model constants and correlation coefficients for adsorption of fluoride onto nano-AlOOH.

Freundlich			Langmuir		
K_f (mg/g)	N	R^2	q_m (mg/g)	b (L/mg)	R^2
20.75	3.50	0.9778	62.50	0.225	0.9822
Dubinin-Radushkevich			Temkin		
q_s (mg/g)	E, kJ/mol	R^2	K_T (l/mg)	RT/b_T	R^2
112.80	13.15	0.9754	92.75	0.00056	0.9614

The equilibrium adsorption isotherm models of the Langmuir, Freundlich, D-R, and Temkin, equations were used to fit the batch experimental data in order to understand the mechanism of fluoride adsorption at the surface of nano-AlOOH. Isotherm parameters and the correlation coefficients (R^2) obtained from the linear curves of each isotherm model are summarized in Table 2.

Therefore, in view of value of R^2 , within the concentration range studied, the Langmuir isotherm presented the experimental data for fluoride adsorption with the highest correlation coefficient value, i.e. the experimental fluoride adsorption data well fitted to Langmuir isotherm. As a result, the Langmuir isotherm provides a good model for this

sorption system and the condition for the validity of a Langmuir isotherm is the model for adsorption on homogeneous surfaces. Moreover, consideration of the comparative magnitudes of the R^2 values, suggest that the Temkin and D-R isotherm produce reasonable fit to the experimental data for F^- ions sorption system onto AlOOH.

3.8 Adsorption Kinetics of Fluoride

The fluoride adsorption kinetics of adsorbent was studied for each initial fluoride concentrations of 40.0, 20.0 and 10.0 mg/L with the corresponding adsorbent dose of 1.6, 0.8 and 0.4 g/L, respectively. The residual fluoride concentrations as a function of time are shown in Fig. 13. The kinetic analysis of the adsorption data is based on reaction kinetics of pseudo first order (result was not shown) and pseudo second order mechanisms.

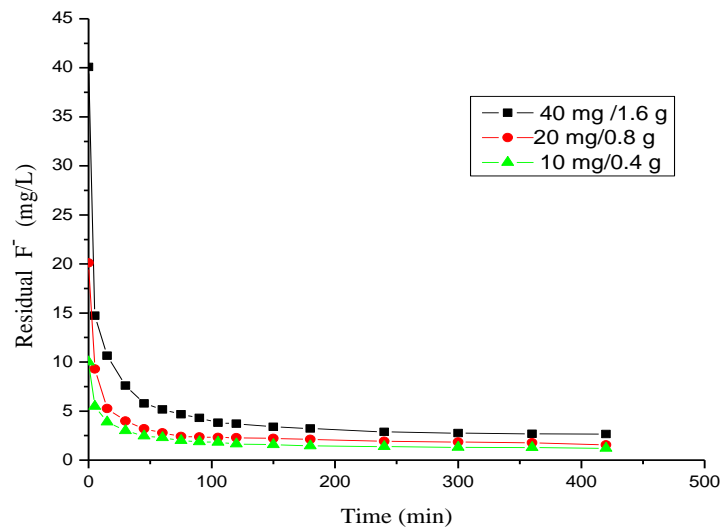


Fig. 13. Adsorption kinetics of fluoride on nano-AlOOH adsorbents at constant surface loading 25 mg/g (average pH = 7).

As indicated from Fig. 13, initially the rates of adsorption of fluoride onto the adsorbent were very fast and then slow down. The changes in the rate of fluoride up take may be due to the fact that, initially, all adsorbents sites were unoccupied and the fluoride concentration gradient was high. Thereafter the fluoride uptake rate by the adsorbents decreased significantly due to the decreased in active sorption sites. The adsorption of fluoride from water is relatively more rapid when the solution is more diluted as can be seen from Fig. 13.

The kinetic analysis of the adsorption of fluoride on the adsorbents was studied based on reaction kinetics of pseudo-second-order mechanisms by using the Lagergren rate equation as shown below:

$$\frac{dq_t}{dt} = k_2(q_e - q_t)^2 \quad (19)$$

$$\frac{d(q_e - q_t)}{(q_e - q_t)^2} = -k_2 dt \quad (20)$$

For the boundary conditions $t = 0$ to $t = t$ and $q_t = 0$ to $q_t = q_t$, the integrated form of Eq. (20) becomes:

$$\frac{1}{(q_e - q_t)} = \frac{1}{q_e} + k_2 t \quad (21)$$

Thus, this is the integrated rate law for a pseudo second-order reaction, Eq. (21) and can be rearranged to obtain Eq. (22), which has a linear form:

$$\frac{t}{q_t} = \frac{1}{k_2 q_e^2} + \frac{t}{q_e} \quad (22)$$

Where q_e and q_t = amount of adsorbed fluoride at equilibrium and any time t (mg/g), K_2 ($\text{g mg}^{-1}\text{min}^{-1}$) = equilibrium rate constant of second-order sorption and t = the contact time (min).

The rate constant can be determined by plotting t/q_t vs. t based on equation above. The larger k_2 value, the slower the adsorption rate. Fig. 14 shows the pseudo-second-order plot of fluoride adsorption kinetics on the adsorbent at three different initial fluoride concentrations for each adsorbent with the same load (25 mg/g). Since the rate constants for the three initial fluoride concentration of each adsorbent were close to each other. Thus the three rate constants of an adsorbent averaged to get a single rate constant, and the correlation coefficients were found as near to unity for the different initial fluoride concentrations as shown in Fig. 15.

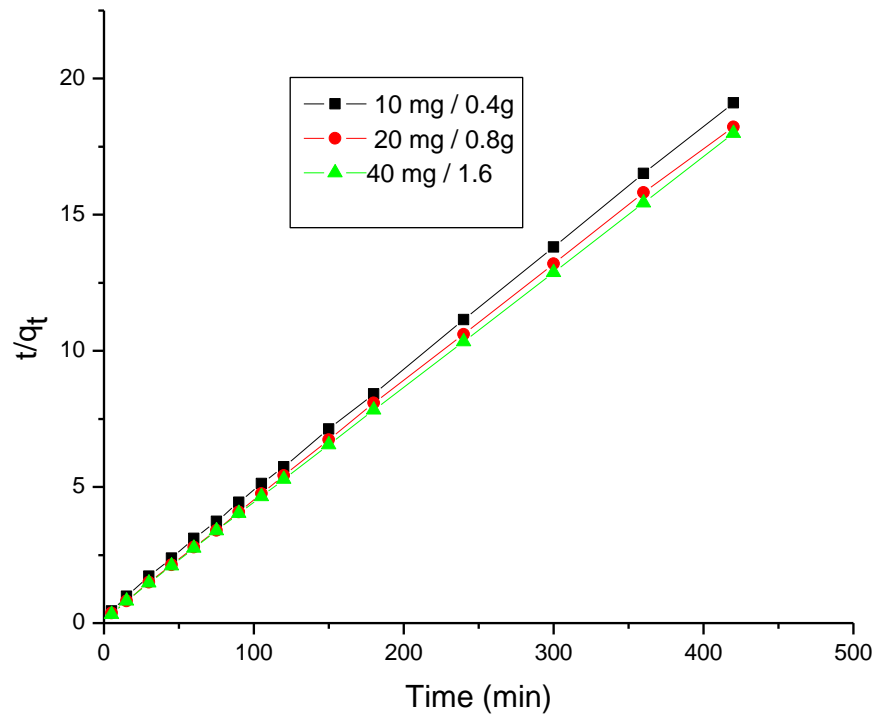


Fig. 14. Pseudo-second-order plot of fluoride adsorption kinetics on adsorbents of different dose each with C_0 to adsorbent dose of 40, 20 and 10 mg/L, and 1.6, 0.8 and 0.4 g/L, respectively (with pH of 7.01 - 7.18).

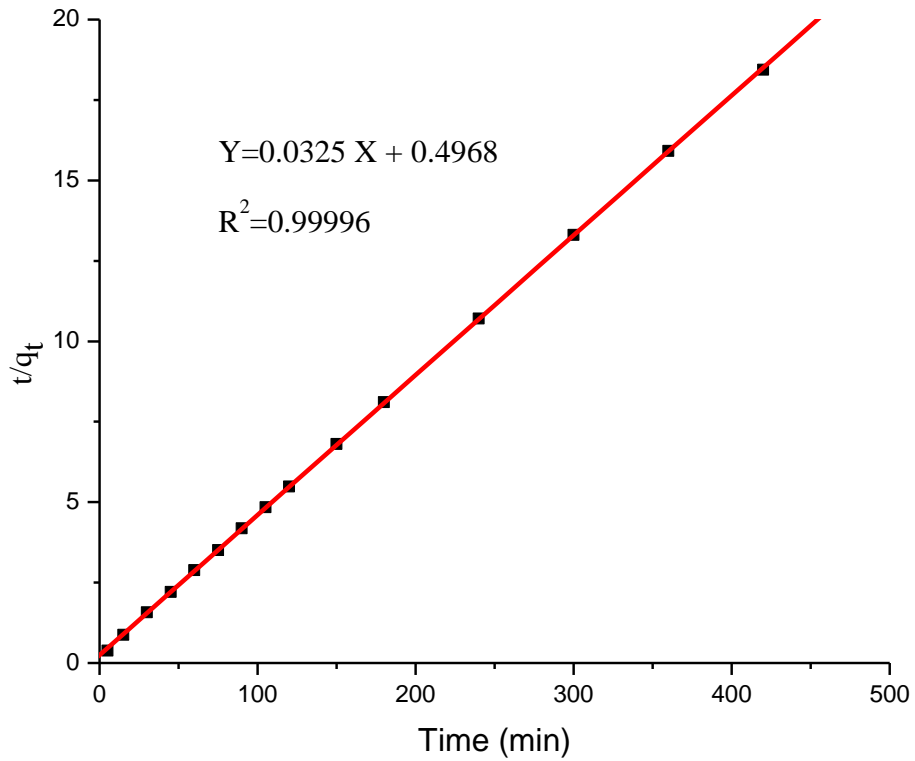


Fig. 15. Average pseudo-second-order plot of fluoride adsorption kinetics on adsorbents each with the same initial load (pH = 7.01-7.18, contact time = 10 h).

Table 3. Summary of the Pseudo-second-order rate constants and correlation coefficients.

Adsorbate (mg/L)/adsorbent(g/L)	Rate constant (k_2)(g $\text{min}^{-1} \text{mg}^{-1}$) ($\times 10^{-3}$)	Rate equation	R^2
10 mg/ 0.4 g	2.030	$t/q_t = 0.0338t + 0.5625$	0.99996
20 mg/ 0.8 g	2.243	$t/q_t = 0.0324t + 0.4651$	0.99995
40 mg/ 1.6 g	2.116	$t/q_t = 0.0313t + 0.4629$	0.99997
Average	2.220	$t/q_t = 0.0325 t + 0.4968$	0.99996

3.9 Intra-particle Diffusion

Adsorption is a surface phenomenon, but the adsorbate may also diffuse into the interior pores of the adsorbent, which may influence the rate of the reaction. Thus the result also analyzed in terms of intraparticle diffusion model to investigate whether the intraparticle diffusion was the rate controlling step in adsorption of fluoride on nano-AlOOH. The amount of fluoride sorbed per unit mass of adsorbents, q_t at any time t , was plotted as a function of square root of time, $t^{1/2}$. The model used here was proposed by Weber and Morris (1963). The linear form of the equation is represented by:

$$q_t = k_d t^{1/2} \quad (23)$$

Where, q_t is the amount adsorbed (mg/g) at time t and k_d ($\text{mg/g min}^{1/2}$) is the intra-particle diffusion rate constant which was obtained using the equation.

If plot of q_t versus $t^{1/2}$ gives a straight line that pass through the origin, then it suggests that the intra-particle diffusion contributes predominantly in the rate-determining step (Ghorai and Pant, 2005). However, if the data exhibit multi-linear plots, then it is anticipated that other mechanisms are also involved along with intra-particle diffusion.

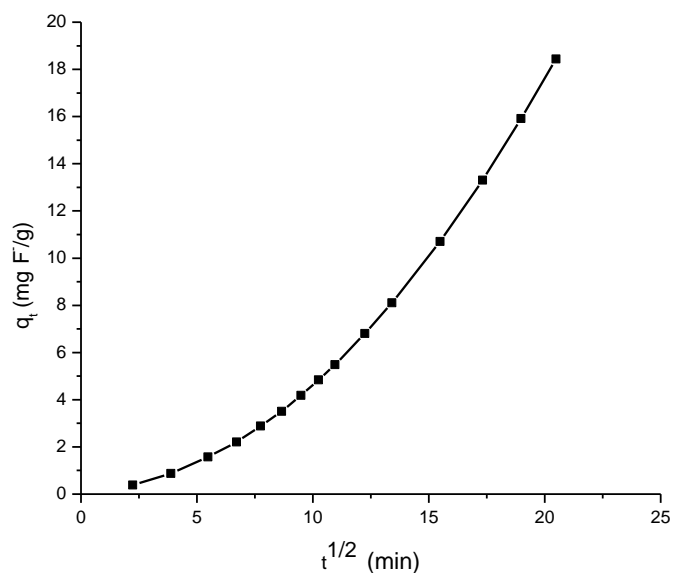


Fig. 16. Weber and Morris intra-particle diffusion plot for the removal of fluoride by nano-AlOOH.

Thus as can be shown in Fig. 16 different regimes can be identified which indicates different mechanisms. The instant initial linear and subsequent curved portion reflects the external surface adsorption and film or boundary layer diffusion effect. The last sharp linear portion of the plot attribute to the intraparticle diffusion effect and the equilibrium uptake. Under this condition, the diffusive transport of fluoride ions occurs through the internal pores of the adsorbent when the bulk fluoride concentration becomes low (Sheta Alemu, 2009). Based on the result it may be concluded that the adsorption mechanism of fluoride ion by nano-AlOOH from aqueous solution is complex process and the intra-particle diffusion was not the only rate-controlling step. Since, the linear portion of the curve does not pass the origin and this result is consistent with the work of Meenakshi *et al.* (2008) and Sundaram *et al.* (2009).

3.10 Mechanism of Adsorption

To further investigate the interactions between fluoride ion and nano-AlOOH the change in pH during the adsorption process was studied after the addition of F^- solutions to properly equilibrate with adsorbent. The pH change studies were conducted at different initial pH by measuring the final pH after adsorption. The initial pH selected was 3, 5, 6, 7, 8, 9 and 10. As shown in Table. 4, the pH of the solution after the sorption reaction increased for a solution with initial pH of the solution below 8. However, for initial pH of solution greater than or equal to 8 the final pH became decreased after the sorption process. Thus adsorption of fluoride at initial pH below 8 might be takes place by ion exchange reaction i.e. due to the replacement of hydroxide ion (OH^-) by fluoride ion (F^-) as shown equation. (24). This is evident from the rise of pH. The result is also in agreement with the proposed adsorption mechanism, in discussion under the D-R isotherm test for adsorption energy value, is chemical ion exchange in nature. If the magnitude of free energy of adsorption is between 8 and 16 kJ/mol, the adsorption process corresponds to chemical in nature (ion exchange).

On the other hand adsorption of fluoride at an initial $pH \geq 8$, the surface slowly acquires negative charges which would repel fluoride ions and hence the fluoride removal by electrostatic attraction is ruled out in alkaline medium. Thus the sorption might be take place by physical sorption process. Since, nano-AlOOH has a pH_{pzc} of 7.8, which means that the surface of the adsorbent presents a net negative charge when $pH \geq 7.8$ (Wang *et al.*, 2008). Therefore, at $pH \geq 8$ nano-AlOOH may function, as a cation exchanger and adsorbs the sodium ions present in solution and releasing protons, which is evident for the resulting decrease in final pH as shown equation. (25) (Wang *et al.*, 2008). On the

basis of other former studies and the result from pH effect study in acidic range, the increase in adsorption efficiency and decrease in final H^+ ion concentration, the adsorption process may follow an ion exchange as the major adsorption mechanism. Thus the most probable mechanism operating for fluoride adsorption by nano-AlOOH can be depicted as follows (Wang *et al.*, 2008; Parida *et al.*, 2009).



Therefore, it can be concluded that fluoride removal by nano-AlOOH is governed by both adsorption and ion exchange mechanism.

Table 4. Change in pH after adsorption process. ($C_0 = 20$ mg/L, contact time = 1 h, dose = 1.6 g/L).

Initial pH of the solution	Final pH of the solution	ΔpH
3	4.55	+ 1.55
5	6.27	+ 1.27
6	6.86	+ 0.86
7	7.32	+ 0.32
8	6.59	- 1.41
9	7.38	- 1.62
10	7.69	- 2.31

3.11 Thermodynamics of Adsorption

The thermodynamic parameters reflect the feasibility and spontaneous nature of the process. Thermodynamic parameters, such as free energy change (ΔG), enthalpy change (ΔH) and entropy change (ΔS) can be estimated using equilibrium constants changing with temperature. The sorption process of F^- on nano-AlOOH can be summarized by the following reversible process, which represents a heterogeneous equilibrium.



The apparent equilibrium constant (K_c) of the sorption is defined as:

$$K_c = \frac{C_{ad,eq}}{C_{eq}} \quad (27)$$

Where, $C_{ad, eq}$, C_{eq} is the concentration of fluoride on the adsorbent and in the solution at equilibrium respectively (Zumriye *et al.*, 2006)

Increase in temperature affects the solubility and chemical potential of the sorbate, which can be a decisive factor for sorption. The dependence of temperature on sorption of F^- ions onto AlOOH was evaluated using the following equation (Mubeena *et al.*, 2006).

$$\ln K_c = -\frac{\Delta H}{RT} + \frac{\Delta S}{R} \quad \text{and} \quad (28)$$

$$\Delta G_o = -RT \ln K_c \quad (29)$$

Where, ΔH (kJ/ mol), ΔS (J/K.mol), ΔG_o (kJ/mol) and T are the enthalpy, entropy, standard Gibbs free energy and temperature (K), respectively, R is universal gas constant and K_c is the equilibrium constant. The thermodynamic parameters can be estimated from the slope and intercept of the linear plots of $\ln K_c$ versus $1/T$ (Fig. 18).

Fig. 17 shows the removal efficiency of fluoride ion as a function of temperature. As can be seen, the removal efficiency increased with increase in temperature. This can be also seen from the positive value of ΔH for fluoride ion adsorption, that is the endothermic nature of the adsorption for the given temperature range. Moreover, the large value of enthalpy showed the strong interaction between the F^- ions and the adsorbent surface which might be due to chemical adsorption. The magnitude of Gibbs free energy for the

sorption process was obtained as in the range of (6.93 – 8.21 kJ mole⁻¹) using equation. (29). A negative value of ΔG_o confirms the feasibility of the process and spontaneous nature of sorption with a high degree of affinity of the fluoride ion for the adsorbent surface. As shown in Fig. 18 the enthalpy and entropy changes of sorption determined from the $\ln K_c$ versus $1/T$ plot ($R^2 = 0.9888$) were 14.51 kJ/mole and 73.37 J/mole.K, respectively.

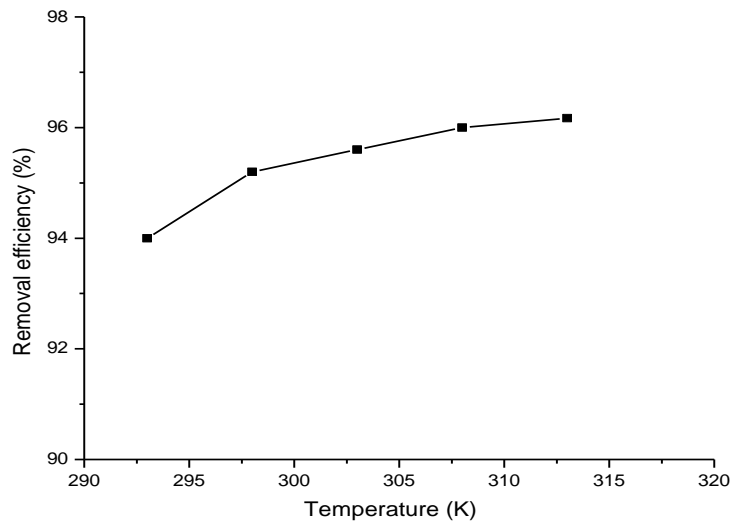


Fig. 17. Effect of temperature on the removal efficiency of fluoride ion onto nano- $AlOOH$ (Dose = 1.6 g/L, $C_o = 20$ mg/L, time = 1 h and pH = 7).

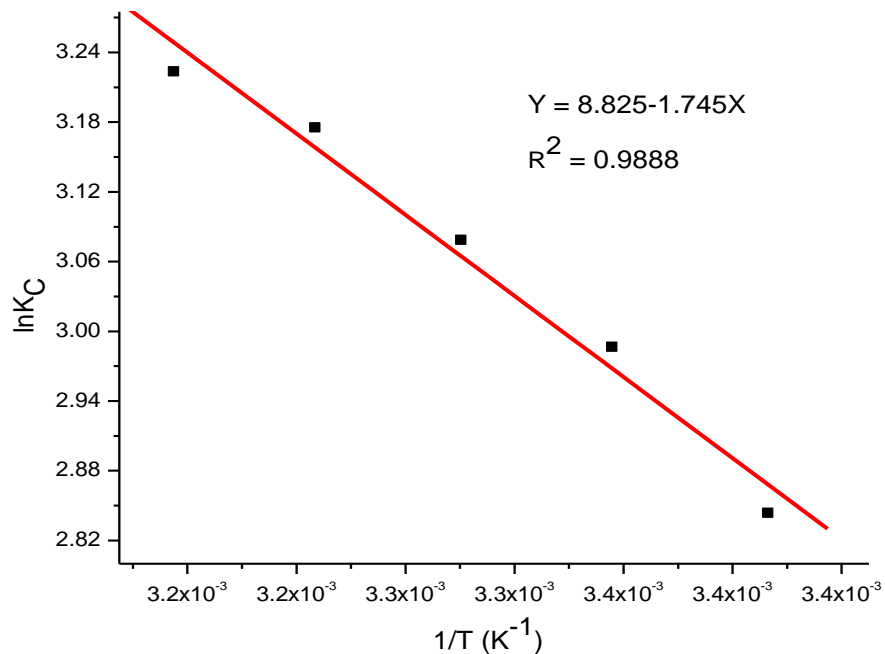


Fig. 18. Variation of equilibrium constant of fluoride ion sorption with temperature (293 - 313 K) (Dose = 1.6 g/L, $C_0 = 20$ mg/L, contact time = 60 min, pH = 7).

The positive value of ΔH_0 indicates an endothermic sorption reaction favorable at higher temperature and comparable with the energy value from D-R isotherm model. The positive value of ΔS° indicates the prevalence of a high degree of disorderliness at the solid-solution interface (the freedom of fluoride ions is not too restricted in the sorbent) during the adsorption process (Sundaram *et al.*, 2009). Therefore, the increase in temperature might have positive role to enhance the adsorption efficiency by causing increased in collision between the fluoride ions and the adsorbent sites (Karthikeyan and Ilango, 2007; Karthikeyan and Elango, 2008). The calculated thermodynamic parameters are presented in Table 5.

Table 5. Thermodynamic parameters for sorption of F⁻ ion onto AlOOH that are computed from the linearized plot of ln K_c versus 1/T at different temperature.

ΔS (J/mol.K)	ΔH (kJ/mol)	ΔG (kJ/mol)					R^2
73.37	14.51	293.15K	298.15K	303.15K	308.15K	313.15K	0.9888
		-6.93	-7.24	-7.59	-7.95	-8.21	

Based on the thermodynamic parameter value, adsorption of fluoride by nano-AlOOH is more endothermic and spontaneous process as compared to nano hydroxyapatite ($\Delta H=7.63$ kJ/mol, $\Delta S = 8.71$ J/mol.k and $\Delta G = -4.73$ kJ/mol) (Sundaram *et al.*, 2008)

3.12 Comparison of Defluoridation Capacities with Other Adsorbents

The fluoride ion adsorption capacity of different sorbent vary according to the nature of the sorbent, since it depends on the affinity of each sorbent to fluoride ions. Thus comparison of defluoridation capacity of different sorbents is fundamental to evaluate their relative potential and for the selection of adsorbents as a defluoridating agent. Hence the adsorption capacity of few sorbents was compared, which are investigated by different studies. The optimum contact time required for the adsorption of fluoride (equilibrium time) was also compared as indicated in Table 6.

Table 6. Defluoridation capacities and optimum contact time required for the adsorption of fluoride by different sorbents.

Adsorbents	Adsorption capacity (mg/g)	Equilibrium time (h)	References
AA (grade A – 25)	1.78	6	Ghorai and Pant, 2005
AA (grade: AD101-F)	0.415	10	Maliyekkal <i>et al.</i> , 2006
MOCA	1.10	3	Maliyekkal <i>et al.</i> , 2006
MCAA	8.9	3	Tripathy and Raichur, 2008
micro-size AlOOH	23.72	1	Yoseph Abebe <i>et al.</i> , 2007
MOAOH	4.48	2	Sheta Alemu, 2009
Activated-carbon oxidized by KMnO ₄	4.54	3	Daifullahand Yakout 2007
Activated kaolinites	0.083	0.5	Meenakshi <i>et al.</i> , 2008
Nano hydroxy apatite	0.706	0.5	Sundaram <i>et al.</i> , 2008
Nano-AlOOH	1.083	6	Wang <i>et al.</i> , 2008
Nano-AlOOH	20.75	1	The present work

MCAA = manganese dioxide-coated activated alumina

MOCA = manganese oxide-coated alumina

MOAOH = Manganese oxide modified aluminum oxide hydroxide

The adsorptive capacity of nano-AlOOH to remove fluoride has been compared with those of other adsorbents reported in the literature (Table 6) based on Freundlich isotherm model. It can be seen that nano-AlOOH exhibits considerably greater F⁻ adsorption potential as compared to other adsorbents except micro-sized AlOOH. It is important to emphasize that the particle size, surface area, surface properties, coordination etc., get modified when material dimensions reach to nano scale. Thus compared with the traditional micron-sized materials used for sorption processes, nano sized carriers' possess a good performance due to high surface area to volume ratio and absence of internal diffusion resistance (Wang *et al.*, 2008).

Therefore, as clearly shown in Table 6 nano-AlOOH has a much higher defluoridation capacity and lower contact time for maximum fluoride adsorption than the other adsorbents except AlOOH reported by Yoseph Abebe *et al.* (2007). However, this compound (micro-sized AlOOH) is not pure compound compared to nano-AlOOH, comprised AlOOH as a major component and trace metal oxides such as, FeO(OH), Fe(OH)₂, Al₂O₃ (Yoseph Abebe *et al.*, 2007). Thus the presence of these oxide compounds may be contributed to its high removal capacity. On the other hand the adsorption coefficient, *b* that is related to the apparent energy of sorption for F⁻ onto nano AlOOH is 0.225 L/mg and that of AlOOH is 0.211 L/mg. This observation showed that the energy of adsorption onto micro-sized AlOOH is lower than that of nano-AlOOH which is probably due to the less affinity of the sorbent on the adsorbate. Since, the higher value of *b* is the strong affinity of the sorbent for the sorbate. Hence, even though the adsorption capacity of nano and micro-sized AlOOH are comparable the binding energy of nano-AlOOH is better than micro-sized one. This shows that the strong affinity of the adsorbent for the adsorbate and regulate the release of fluoride ion after sorption to the treated water.

When capacity and equilibrium time are taken consideration as a criterion to make selection among the adsorbents listed above, use of nano-AlOOH as a defluoridation media is preferable than the other adsorbents except micro size AlOOH. Moreover, in this study the capacity of nano-AlOOH and equilibrium time for adsorption of fluoride improved as compared to the result of Wang *et al.* (2008). Therefore, comparison of defluoridation capacities, equilibrium sorption time and adsorption kinetics F⁻ onto nano-

AlOOH the present work provide better outcome than the result reported by Wang *et al.* (2008).

4. Conclusion and Recommendation

Nano-AlOOH has considerable potential for the removal of excess fluoride from aqueous solution. For a given initial fluoride concentration, the removal efficiency of the adsorbent increased with increasing adsorbent dose. Adsorption of fluoride is very rapid in the first 30 min and then increases slowly to reach pseudo-equilibrium. Thermal treatment of the sorbent at temperature of 200 °C slightly increased the fluoride removal efficiency and selected for further study. Initial concentration of fluoride also found to affect the defluoridation efficiency of the adsorbent. Solution pH is the most important parameter affecting adsorption capacity of the adsorbents. Although high fluoride removal occurred between pH 6 to 8, appreciable amount of fluoride was removed around pH 7. The equilibrium data were tested to fit Freundlich, Langmuir, D-R and Temkin isotherm models in order to understand the mechanism of fluoride adsorption at the surface of AlOOH. Therefore, the Langmuir isotherm model corresponded to better with the experimental equilibrium data, and the maximum adsorption capacities; q_m of the adsorbent was 62.50 mg/g. The D-R model gave adsorption energy, 13.15 kJ/mole which indicates the fluoride removal by nano-AlOOH is chemisorptions process. Adsorption kinetics followed and well described by a pseudo-second order model. Intra-particle diffusion was not the rate controlling step during the adsorption process. The mechanism of the adsorption process on the basis of change in pH after adsorption process and the free energy value from D-R model (13.15 kJ/mol) was an ion exchange

mechanism. The thermodynamic studies revealed from the value of ΔH , ΔS and ΔG adsorption of fluoride by nano-AlOOH were an endothermic and spontaneous process.

Comparison of adsorption capacity and contact time required for maximum adsorption of fluoride (equilibrium time) with other some sorbents, nano-AlOOH has shown that a better adsorption potential and performance except AlOOH reported by Yoseph Abebe et al. (2007). Thus, nano-AlOOH is efficient and very promising adsorbent with reasonable defluoridation Capacity, and could be considered as in finding appropriate sorbent for a sustainable solution to mitigate the fluoride problem in the country.

In view of the fact that most of the rural populations in the Rift Valley Region of the country cannot afford treated water for their daily consumption. Thus this efficient material has to be considered to establish a sustainable solution to the fluoride problem in the Rift Valley Region of Ethiopia. Hence from this study a promising result is obtained regarding the efficiency of the adsorbent.

Thus the removal of fluoride using nano-AlOOH in continuous mode has to be practice and the methods has to be optimize for further study by coating the adsorbent with other material or by using supporting bed and can be formed into column. The removal of excess fluorides from community water supplies to prevent dental and skeletal fluorosis should be adopted as fast as possible.

The human curiosity to know the unknown things are the fundamental basis for scientific development. Based on the finding of present investigation and to put practice for further studies the following points should be considered:

- ❖ Further studies on:
 - Further characterizing the adsorbent in detail.
 - The adsorption performance of the adsorbent in continuous operation and optimizing the column experimental parameters.
 - The regeneration of the exhaust adsorbent and safe disposal of the regenerate.
 - Physical, chemical and biological characteristics of treated water.
 - Assessing the efficiency and capacity of the adsorbent with real fluoride contaminated water samples.

References

- Ayoob, S. and Gupta, K. (2006). Fluoride in Drinking Water: A Review on the status and stress effects. *Envi. Sci. and Tech.* **36**:433-487.
- Bache, B. W. and Williams, E. G. (1971). A phosphate sorption index for soils. *J. soil Sci.* **22**:289-301.
- Bailey, P. L. (1980). *Analysis with Ion-Selective Electrodes*, 3rd edition, Heidon, London, p. 196.
- Banerjee, S. S. and Chen, D. H. (2007). Fast removal of copper ions by gum Arabic modified magnetic nano-adsorbent. *J. Hazard. Mater.* **149**:792-799.
- Bardsen, A. and Bjorvant, K. (1997). Fluoride sorption in fired clay. *In Proceeding of the First International Workshop on Fluorosis and Defluoridation of Water*, Tanzania. The International society for Fluoride Research, Auckland. 46-49.
- Beneberu, S., Feleke, Z. and Chandravanshi, B. S. (2006). Removal of excess fluoride from water by aluminum hydroxide. *Bull.chem.Soc.Ethiop.* **20**(1):17-34.
- Boruff, C. S. (1934). Removal of fluorides from drinking water. *Ind.Eng.Chem.* **26**(1):69-71.
- CRC (2008). Cooperative Research Center (CRC) for water Quality and treatment investigation of Defluoridation Options for Rural and Remote Communities. *Research report No 41*, ISBN 18766 166679, Australia.
- Dahi, E. (2000). The State of Art of Small Community Defluoridation of drinking Water. 3rd International Workshop on Fluorosis Prevention and Defluoridation of Water, Chiang, Mai and Thailand. 137-167.
- Daifullah, A. A. and Yakout, S. M. (2007). Adsorption of fluoride in aqueous solutions using KMnO₄-modified activated carbon from steam pyrolysis of rice straw. *J. Hazard. Mater.* **147**:633-643.
- Dissanayake, C. B. (1991). The fluoride problem in the ground water of Srilanka, environmental management and health. *Inter. J. Environ. Study.* **19**:195-203.
- Eva, K., Amit, B., Minkyu, J., Woosik, J., Sang, H. L., Sun, J. K., Giehyeon, L., Hocheol, S., Jae, Y. C., Jung, S. Y. and Byong, H. J. (2009). Defluoridation from aqueous solutions by granular ferric hydroxide (GFH). *Wat. Res.* **43**(2):490-498.

- Fawell, J., Bailey, K., Chilton, J., Dahi, E., Fewtrell, L. and Magara, Y. (2006). Fluoride in Drinking water. WHO and IWA publishing London.
- Feleke, Z. (2001). Investigation leading to the Defluoridation of water in Ethiopia. A report submitted to the Ethiopian science and technology commission (unpublished report), Addis Ababa.
- Federal Democratic Republic of Ethiopia, Ethiopian Quality and Standard Authority guidelines, EQSA. (2001). Addis Ababa, Ethiopia.
- Federal Democratic Republic of Ethiopia, MoWR, Ministry of Water resources. (2002). Ethiopian Guidelines Specification for drinking Quality, Addis Ababa, Ethiopia.
- Girma, M., Feleke, Z. and Scoher, M. (1996). Preliminary investigation on defluoridating of water using fired clay chips. *J. Afr. Ear. Sci.* **21**(4):479-482.
- Gopalan, V., Jaswanth, A., Gopalakrishan, S. and Sivailango, S. (2009). Mapping of fluoride endemic areas and assessment of fluoride exposure. *Sci. Total. Environ.* **407**:1579-1587.
- Ghorai, S. and Pant, K.K. (2005). Equilibrium, Kinetics and break through studies for adsorption of fluoride on activated carbon. *Sep. Puri. Technol.* **42**:265-271.
- Hao, O. Asce, A., Huang, C. and Asce, M. (1986). Adsorption characteristics of Fluoride onto Hydrous Alumina. *J. Environ.* **112**(6):1054-1069.
- He, G. L. and Cao, S. R. (1996). Assessment of fluoride removal from drinking water by calcium phosphate systems. *J. Fluor.* **29**:212-216.
- Hobson, J. P. (1969). Physical adsorption isotherms extending from ultrahigh vacuum to vapor pressure. *J. Phys. chem.* **73**:2720-2727.
- Hochepped, J. F., Ilioukhina, O. and Berger, M. H. (2003). Effect of the mixing procedure on aluminum oxide hydroxide obtained by precipitation of aluminum nitrate with soda. *Mater. Letters.* **57**(19):2817-2822.
- IPCS (2002). Fluorides. World Health Organization, International Programme on chemical Safety, Safe water Technology for Arsenic removal report.
- ISDWS (1996). Indian Standard: Drinking Water-Specifications, IS: 10500:1991, New Delhi.
- Jamode, A. V., Spakal, V. S., Jamode, V. S. (2004). Defluoridation of water using Inexpensive Adsorbents. *J. Ind. Inst. Sci.* **84**:163-171.

- Karthikeyan, G., Ilango, S.S. (2007). Fluoride Sorption Using Moringa Indica –Based Activated Carbon. *Iran. J. Environ. Health Sci. Eng.* **4**(1):21-28.
- Karthikeyan, M. and Elango, K.P. (2008). Removal of Fluoride from aqueous solution using graphite: A kinetics and thermodynamics study. *J. Ind. Chem. Technol.* **15**:525-532.
- Kiran, I., Akar, T., Ozcan, A.S., Ozcan, A., Tunali, S. (2006). Biosorption kinetics and isotherm Studies of Acid 57 by dried *Cephalosporium aphidicola* cells from aqueous solutions. *J. Biochem. Eng.* **31**:199-200.
- Kloos, H., and Teklehaimanot, R. (1999). Distribution of fluoride and fluorosis in Ethiopia and prospects for control. *Trop. Med. Int. Health* **4**(5):355-364.
- Maliyekkal, S.M., Sharma, A.K., Philipet, L. (2006). Manganese-oxide- coated alumina: A promising sorbent for defluoridation of water. *Wat. Res.* **40**:3497-3506.
- Meenakshi, S., Sundaram, C. S. and Sukumar, R. (2008). Enhanced fluoride sorption by mechanochemically activated Kaolinites. *J. Hazard. Mater.* **153**(1-2):164-172.
- Min, B. R., Gill, A. L. and Gill, W. N. (1984). A Note on Fluoride removal by Reverse Osmosis. *J.Desalination.* **49**(1):89-105.
- Mubeena, A., Syed, M., Bhangar, M. and Shahid, I. (2006). Low cost sorbent for the removal of methyl parathion pesticide from aqueous solution. *J.Chem.***9**:61-72.
- Murray, J.J. (1986). Appropriate use of Fluorides for Human Health. World Health Organization, Geneva.
- Nalan, K., Ozgur, A., Saba, S., Umran, Y. and Mithat, Y. (2008). Separation of fluoride from aqueous solutions by electrodialysis: Effect of process parameters and other ionic species. *J. Hazard. Mater.* **153**:107-113.
- Nawlakhe, W. G., Kulkarni, D. N., Pathak, B. N. and Bulusu, K. R. (1974). Defluoridation of water with alum. *Ind. J. Environ. Health* **16**(1):156-168.
- Nawlakhe, W. G., Kulkarni, D. N., Pathak, B. N. and Bulusu, K. R. (1975). Defluoridation of water by Nalgonda technique. *Ind. J. Environ. Health* **17**:26-65.
- Nemade, P. D., Rao, A. V. and Alappat, B. J. (2002). Removal of fluoride from Water Using Low cost Adsorbents. *Wat. Sci. Technol.* **2**:311-317.
- Olsson, B. (1979). Dental finding in high fluoride area in Ethiopia. *Dent. Oral Epidemiol.* **7**:51-56.

- Parida, K. M., Amaresh, C. P., Das, J. and Naruparaj, S. (2009). Synthesis and Characterization of nano-sized porous gamma-alumina by control precipitation method. *J. Mater. Chem. Phys.* **113** (1):244-248.
- Pietrelli, L. (2005). Fluoride waste water treatment by Adsorption on to Metallurgical Grade Alumina. *Ann. Chim.* **95**:303-312.
- Reimann, C., Bjorvatn, k., Frengstad, B., Zeneb, M., Redda, T. and Siewers, U. (2003). Drinking water quality in the Ethiopian section of the east African Rift Valley I- data and health aspects. *Sci. Total Environ.* **311**:65-80.
- Rieman, W. and Walton, H. (1970). Ion Exchange in Analytical chemistry, in International Series of Monographs in Analytical Chemistry, Vol. 38, Pergamon, Oxford.
- Sanjeev, S., Rohini, J., Naveen, S. M. and Mahesh, S. (2009). Electrocoagulation Using DC Current for Removal of fluoride from Ground water. Proceedings of international conference on energy and environment. 2070-3740.
- Sheta, A. (2009). Investigation of Fluoride Adsorption on Manganese Oxide Modified Aluminum Oxide Hydroxide. Master's thesis of Environmental science program, Addis Ababa University, Ethiopia.
- Shrivastava, B. K. and Vani, A. (2009). Comparative study of Defluoridation technologies in India. *Asian. J. Exp. Sci.* **23**(1):269-274.
- Srimurali, M., and Karthikeyan, J. (2008). Activated Alumina: Defluoridation of Water and house hold application a study. Twelfth International Water Technology Conference, IWTC12: Alexandria, Egypt. 153-165.
- Stefansson, A. Gunnarsson, I., and Giroud. N. (2007). New methods for the direct determination of dissolved inorganic, organic and total carbon in natural waters by Reagent-Free Ion Chromatography and inductively coupled plasma atomic emission spectrometry". *Anal. Chim. Acta* **582** (1): 69–74.
- Sundaram, C. S., Viswanathan, N. and Meenakshi, S. (2008). Defluoridation chemistry of synthetic hydroxyapatite at nano scale: equilibrium and kinetic studies. *J. Hazard. Mater.* **155**:206-215.
- Sundaram, C.S., Viswanathan, N. and Meenakishi, S. (2009). Fluoride sorption by nano-hydroxyapatite /Chitin composite. *J.Hazard. Mater.* **172**(1):147-151.

- Symonds, R. B., Rose, W. I. and Reed, M. H. (1988). Contribution of chlorine and fluorine gases to the atmosphere by volcanoes. *Nature* **334**:415-418.
- Tahaikt, M., Habbani, R., Eli, H., Ait, A., Achary, I., Amazor, Z., Taky, M., Alami, A., Boughriba, A., Hafsi, M. and Elmidaoui, A. (2007). Fluoride removal from ground water by nanofiltration. *J. Desal.* **212**:46-53.
- Tandada, S., Kabayama, M., Kawasaki, N., Sakiyama, T., Nakamura, T., Araki, M. and Tamura, T. (2003). Removal of Phosphate by aluminum oxide hydroxide. *J. Coll. Inter. Sci.* **257**:135-140.
- Tebutt, T. (1983). Relationship between Natural Water Quality and Health. United Nations Educational, Scientific and Cultural Organization, Paris.
- Teklehaimanot, R., Fekadu, A. and Bushura, B. (1987). Endemic fluorosis in the Ethiopian Rift valley. *Trop. Geog. Med.* **39**:209-217.
- Tripathy, S. S. and Richur, A. M. (2008). Abatement of fluoride from water using manganese dioxide-coated activated alumina. *J. Hazard. Mater.* **153**(3):1043-1051.
- USEPA, Environmental Protection Agency. (1986). Fluoride in Drinking Water: A Scientific Review of EPA's Standards. USEPA.
- Venkobachar, C., Leela, L. and Mudgal, A. K. (1997). Household Defluoridation of Drinking Water Using Activated Technology, *2nd International Workshop on Fluorosis and Defluoridation of Water, Nazereth, Ethiopia.*
- Wang, S. G., Yue, M., Yijing, S. and Wen, X. (2008). Defluoridation performance and mechanism of nano scale aluminum oxide hydroxide in aqueous solution. *Whiley inter science. J. Chem. Techn. Biotechn.* 45-52.
- Weber, T. W. and Chakkravorti, R. (1974). Pore and solid diffusion models for fixed bed absorbers. *J. Alche.* **20**:228.
- Weber, W.J., Morris, J.C., (1963). Kinetics of adsorption of carbon from solution. *J. Sanit. Eng. Div. ASCE.* **89**, 31-59.
- Wefers, K. and Misra, C. (1987). Oxides and Hydroxides of Aluminum, Alcoa Technical Paper No.19.
- WHO (1970). World Health Organization, Fluorides and human health. WHO Monograph series, Geneva. No.59.

- WHO (1984). Guidelines for Drinking water Quality Vol.1 and 2, Geneva, Switzerland.
- WHO (1999). World Health Organization, Fluoride in Drinking Water, Geneva.
- WHO (2004). Guidelines for drinking water quality 3rd edition, World Health Organization, Geneva, 301-303,375-378.
- WHO (2004b). *Fluoride in Drinking-water: Background document for development of WHO Guidelines for Drinking-water Quality* WHO/SDE/WSH/03.04/96. World Health Organization, Geneva, Switzerland.
- Worku, N., Feleke, Z. and Chandravanshi, B.S. (2007). Removal of excess fluoride from water using waste residue from alum manufacturing process. *J. Hazard. Mater.* **147**(3):954-963.
- Yoseph, A., Feleke, Z. and Chandravanshi, B. S. (2007). Fluoride removal from water with Aluminum oxide hydroxide: a pilot study for household application. Master's thesis Environmental science program, Addis Ababa University.
- Zevenbergen, C., Van Reeuvijk, L.P., Louws, R.J. and Schiling, R.D. (1996). A simple method for Defluoridation of drinking water at village level by adsorption on ando soil in Kenya. *Sci. Total. Environ.* **188**:225-232.
- Zumriy, A., Seyda, S. and Cagatay, C. (2006). Investigation of biosorption of Gemoazol Turquoise Blue-G reactive dye by dried *Rhizopus arrizus* in batch and continuous system. *Sep. Puri. Technol.* **48**: 24–35.